Atmospheric Environment 191 (2018) 513–524

Contents lists available at ScienceDirect

Atmospheric Environment

journal homepage: www.elsevier.com/locate/atmosenv

Observations of Manaus urban plume evolution and interaction with biogenic emissions in GoAmazon 2014/5

Glauber Cirino[a,b,*], Joel Brito[c,1], Henrique M.J. Barbosa[c], Luciana V. Rizzo[d], Peter Tunved[e], Suzane S. de Sá[f], Jose L. Jimenez[g], Brett B. Palm[g], Samara Carbone[c,2], Jost V. Lavric[h], Rodrigo A.F. Souza[i], Stefan Wolff[j], David Walter[j], Júlio Tota[k], Maria B.L. Oliveira[i], Scot T. Martin[f,l], Paulo Artaxo[c]

[a] Department of Meteorology, Geosciences Institute, Universidade Federal do Pará, Belém, Pará, Brazil
[b] Post-graduate Program in Climate and Environment, National Institute for Amazonian Research and Amazonas State University, Manaus, Amazonas, Brazil
[c] Institute of Physics, University of São Paulo, São Paulo, São Paulo, Brazil
[d] Department of Environmental Sciences, Institute of Environmental, Chemical and Pharmaceutics Sciences, Universidade Federal de São Paulo, São Paulo, São Paulo, Brazil
[e] Department of Environmental Science and Analytical Chemistry, Stockholm University, Stockholm, Sweden
[f] School of Engineering and Applied Sciences, Harvard University, Cambridge, MA, USA
[g] University of Colorado at Boulder, Boulder, CO, USA
[h] Max Planck Institute for Biogeochemistry, Jena, Germany
[i] Department of Meteorology, Amazonas State University, Manaus, Amazonas, Brazil
[j] Max Planck Institute for Chemistry, Mainz, Germany
[k] Institute of Engineering and Geoscience, Federal University of West Para, Santarém, Pará, Brazil
[l] Department of Earth and Planetary Sciences, Harvard University, Cambridge, MA, USA

GRAPHICAL ABSTRACT

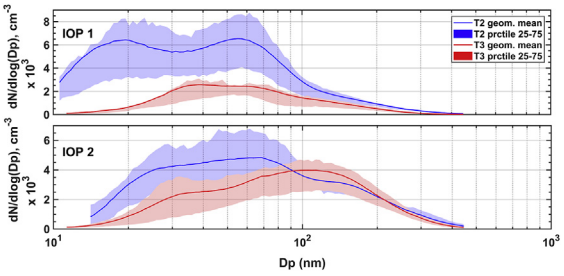

ARTICLE INFO

Keywords:
GoAmazon
Plume aging
Aerosol
Manaus
Tropical forest
Urban pollution

ABSTRACT

As part of the Observations and Modeling of the Green Ocean Amazon (GoAmazon 2014/5) Experiment, detailed aerosol and trace gas measurements were conducted near Manaus, a metropolis located in the central Amazon Basin. Measurements of aerosol particles and trace gases were done downwind Manaus at the sites T2 (Tiwa Hotel) and T3 (Manacapuru), at a distance of 8 and 70 km from Manaus, respectively. Based on in-plume measurements closer to Manaus (site T2), the chemical signatures of city emissions were used to improve the interpretation of pollutant levels at the T3 site. We derived chemical and physical properties for the city's atmospheric emission ensemble, taking into account only air masses impacted by the Manaus plume at both sites, during the wet and dry season Intensive Operating Periods (IOPs). At T2, average concentrations of aerosol number (CN), CO and SO_2 were

* Corresponding author. Department of Meteorology, Geosciences Institute, Universidade Federal do Pará, Belém, Pará, Brazil.
E-mail address: glaubercirino@ufpa.br (G. Cirino).
[1] Now at: Laboratory for Meteorological Physics (LaMP), University Blaise Pascal, Aubière, France.
[2] Now at: Agrarian Sciences Institute, Federal University of Uberlandia, Uberlandia, Minas Gerais, Brazil.

https://doi.org/10.1016/j.atmosenv.2018.08.031
Received 10 February 2018; Received in revised form 9 August 2018; Accepted 13 August 2018
Available online 16 August 2018

5500 cm^{-3} (between 10 and 490 nm), 145 ppb and 0.60 ppb, respectively, with a typical ratio ΔCN/ΔCO of 60–130 particles cm^{-3} ppb^{-1}. The aerosol scattering (at RH < 60%) and absorption at 637 nm at T2 ranged from 10 to 50 M m^{-1} and 5–10 M m^{-1}, respectively, leading to a mean single scattering albedo (SSA) of 0.70. In addition to identifying periods dominated by Manaus emissions at both T2 and T3, the plume transport between the two sampling sites was studied using back trajectory calculations. Results show that the presence of the Manaus plume at site T3 was important mainly during the daytime and at the end of the afternoons. During time periods directly impacted by Manaus emissions, an average aerosol number concentration of 3200 cm^{-3} was measured at T3. Analysis of plume evolution between T2 and T3 indicates a transport time of 4–5 h. Changes of submicron organic and sulfate aerosols ratios relative to CO (ΔOA/ΔCO and $\Delta SO_4/\Delta CO$, respectively) indicate significant production of secondary organic aerosol (SOA), corresponding to a 40% mass increase in OA and a 30% in SO_4 mass concentration. Similarly, during air mass arrival at T3 the SSA increased to 0.83 from 0.70 at T2, mainly associated with an increase in organic aerosol concentration. Aerosol particle size distributions show a strong decrease in the Aitken nuclei mode (10–100 nm) during the transport from T2 to T3, in particular above 30 nm, as a result of efficient coagulation processes into larger particles. A decrease of 30% in the particle number concentration and an increase of about 50 nm in geometric mean diameter were observed from T2 to T3 sites. The study of the evolution of aerosol properties downwind of the city of Manaus improves our understanding of how coupling of anthropogenic and biogenic sources may be impacting the sensitive Amazonian atmosphere.

1. Introduction

The Amazon forest, particularly during the rainy season, has one of the lowest aerosol particle number concentrations in continental areas (Andreae et al., 2015; Artaxo et al., 2013; Scot T. Martin et al., 2010a). Biogenic aerosol particles and trace gases emitted by vegetation are linked to cloud microphysics, precipitation production, atmospheric radiation balance, and nutrient cycling, which in turn may affect complex processes in the ecosystem (Pöschl et al., 2010; Pöhlker et al., 2012; China et al., 2016; Wang et al., 2016; Whitehead et al., 2016a,b; Cecchini et al., 2017).

Since the 1980s, forest fires have been used to clear large portions of the Basin after deforestation, mostly over the so-called deforestation arc, on the Southern and Western Amazon borders. The seasonal biomass burning significantly alters the aerosol loading (Artaxo et al., 2013; Brito et al., 2014) and has significant effects on the net ecosystem exchange of CO_2 (Oliveira et al., 2007; Dougthy et al., 2010; Cirino et al., 2014; Rap et al., 2015), climate (Andreae et al., 2004; Heiblum et al., 2014; Sena et al., 2013) and human health (Oliveira et al., 2015; Reddington et al., 2015). While during recent years the deforestation rate has decreased (Artaxo et al., 2013; Nepstad et al., 2014), the urbanization process in the Amazon basin has increased, and it has been identified as a significant driver of land use change, potentially affecting large areas of the forest (Davidson et al., 2012; Fraser, 2014). Moreover, the effects of increasing urban emissions on climate and air quality, as well as their interactions with biogenic emissions in Amazonia, are still poorly understood. Previous studies indicate that the combination of biogenic or anthropogenic VOCs emissions with urban NO_x and SO_2 emissions can increase tropospheric ozone production (Kuhn et al., 2010; Martin et al., 2016, 2017) and impact the production of secondary aerosols in the region (De Sá et al., 2017; Palm et al., 2018). These secondary aerosols will have an impact on the chemistry of biogenic VOCs and hydroxyl radical (OH) (Liu et al., 2016), thus modifying the chemical composition of the atmosphere in the Amazon. Changes in the optical properties of aerosols due to these interactions can potentially result in significant impacts on the regional carbon balance, with still unknown effects on the ecosystem and regional climate. Also, urban emission amidst a tropical forest environment may impact aerosol chemical and physical properties and alter the natural mechanisms controlling clouds and precipitation processes (Cecchini et al., 2016; Kuhn et al., 2010; Martin et al., 2016).

Understanding the interplay of natural and anthropogenic processes and how they regulate the composition of the atmosphere, is vital for defining sustainable regional development strategies. In this context, the Observations and Modeling of the Green Ocean Amazon (GoAmazon, 2014/5, Martin et al., 2016) experiment conducted a broad set of measurements to better understand the environmental impacts of urban centers on the natural microphysical properties of clouds and aerosols, such as particle size distribution, optical properties, and cloud condensation nuclei (CCN) activity (Thalman et al., 2017), in central Amazon. The experiment took advantage of the geographic location of Manaus city, an isolated urban area of over 2 million people and 600,000 vehicles, growing at a rate of 170% in 10 years, surrounded by forest extending by more than 1000 km in every

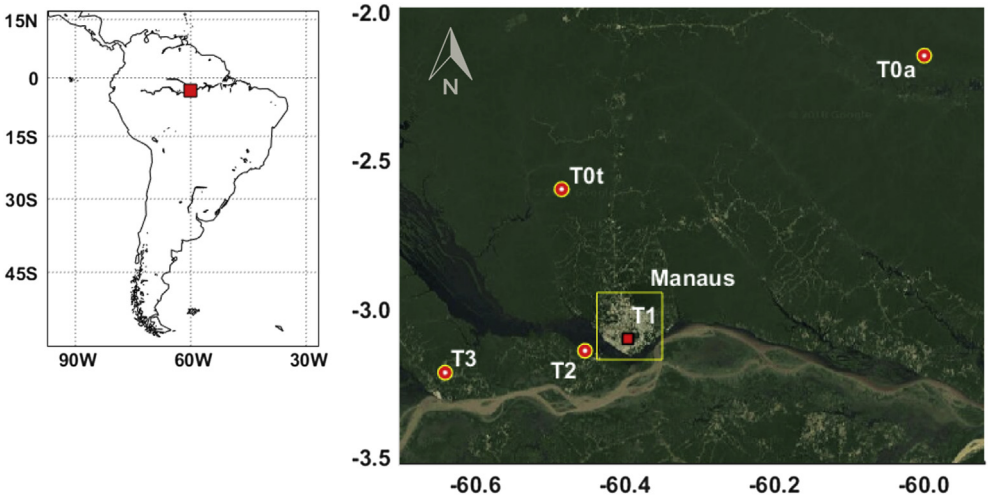

Fig. 1. Location of the sampling site shown by the red marker (left panel) and map showing the GoAmazon 2014/5 sites: T0t (~60 km northwest) and T0a (~150 km northeast), both upwind Manaus; T2 (~8 km) and T3 (~70 km), both downwind of Manaus, Amazonas, Brazil (right panel). (For interpretation of the references to color in this figure legend, the reader is referred to the Web version of this article.)

direction (Martin et al., 2016). Manaus accounts for 80% of the economic activity of the state of Amazonas and its electricity is predominantly produced by the combustion of fossil fuels (Medeiros et al., 2017). The experiment combined aircraft measurements and several ground based sites operating simultaneously to monitor polluted air masses, originating from Manaus urban emissions, as they move over undisturbed forest carried by the prevailing trade winds (Martin et al., 2016).

This study is based on measurements at two GoAmazon 2014/15 ground sites downwind from Manaus and aims to provide a better understanding of the impact of urbanization on the properties of the Amazonian aerosol life cycle. Our analysis of the datasets reveals how chemical and physical properties of aerosols in the central Amazon are impacted by Manaus urban emissions. Our objective is to describe and understand the physical and chemical changes of aerosol particles in the urban plume during transport away from the city, from site T2 to site T3, 8 and 70 km downwind from the city, respectively. Our study contributes to a better understanding of how emissions associated with a rapidly growing metropolitan region affect the aerosol life cycle in the tropics.

2. Methods

2.1. Sites description

The locations of the two GoAmazon 2014/15 sampling sites used in this study, site T2 (3° 8′21.12″S, 60° 7′53.40″W, Tiwa Hotel, Iranduba, Brazil) and site T3 (3° 12′47.88″S, 60° 35′55.32″W, Manacapuru, Brazil) are shown in Fig. 1. Overall, in this region, there is a very little seasonal variation for surface T, RH, and q, as already shown by different authors. For instance, average T in February is 26.5 °C, and 27.8 °C in September. Mixing ratio (q) is 20 g kg^{-1} in April–May, and 19.1 g kg^{-1} in August (Collow et al., 2016). The seasonal cycle of precipitation is driven by the Intertropical Convergence Zone (ITCZ), which provides a wet season (rainfall greater than 200 mm) from January to April and a dry season (rainfall less than 105 mm) from July to September (Da Rocha et al., 2009). Prevailing winds blow typically from the east and northeast (Dos Santos et al., 2014) at low wind speeds of about 2 m s^{-1} (Fig. S1, Supplementary Material). Due to its location, site T2 is heavily impacted by the Manaus urban plume as well as emissions from brick factories and to a minor extent by local pollution sources such as shipping or burning of household waste and wood near the site (Martin et al., 2016). This arises from both its location (with Manaus 8 km to the east and brick factories to the west) and the prevailing easterly wind direction modulated by a significant river breeze (Fig. S1). Site T3 is located 70 km downwind of Manaus, in a pastureland 2 km to the north of road AM-070. More information about the GoAmazon 2014/15 sampling sites can be found in Martin et al. (2016).

The T2 site and its instrumentation were maintained by the University of São Paulo (USP), the National Institute of Amazonian Research (INPA), and Amazonas State University (UEA). Data from the T3 site were obtained from the Mobile Aerosol Observing System (MAOS), maintained by the Atmospheric Radiation Measurement (ARM) Climate Research Facility (DoE, USA). Additional data of particle chemical composition and particles size distribution were obtained from the University of Colorado at Boulder and Harvard University groups (USA) (De Sá et al., 2017). Measurements at sites T0t (TT34, ZF2, 2.6091S 60.2093W) and T0a (ATTO, 2.1441S 58.9999W), 80 km and 150 km upwind of Manaus respectively, provided carbon monoxide (CO) background concentrations. These sites are operated by INPA, UEA, USP, and the Max Planck Institute for Chemistry and Biogeochemistry.

2.2. Instrumentation and measurements

The dataset analyzed here spans both Intensive Operating Periods (IOP), from 1 February to 31 March 2014 in the wet season (IOP 1) and from 15 August to 15 October 2014 in the dry season (IOP 2). All data were averaged to 30 min periods and compensated for standard temperature and pressure (1013.25 hPa; 273.15 K). Aerosols were sampled through a PM_{10} inlet 12 m a.g.l at T2 at a flow rate of 16.7 LPM, using a 1/2-inch copper line. At T3, the PM_{10} inlets coupled to the instruments were respectively 5 m (aerosol chemical speciation) and 10 m (aerosol physical properties) above ground level, both using 1/2-inch copper lines. At both sites, sampling under dry conditions (RH < 60%) was assured by the use of silica diffusion dryers. Trace gases were sampled using 1/4-inch Teflon lines (inlet height 45, 3 and 10 m at T0z, T2 and T3, respectively). Detailed information of AMS and trace gases operation at T3 are presented by De Sá et al. (2017). A similar set of instruments was used at both sites, providing measurements of aerosol scattering and absorption at multiple wavelengths, aerosol number concentration and size distribution, aerosol chemical speciation, and trace gases concentration. Subsections below give additional information on each instrument and data analysis procedures, which are summarized in Table S1.

2.2.1. Meteorological measurements

Meteorological parameters were measured using two different Automatic Weather Stations (AWS) models: U30 Station GSM-UDP (HOBO) and WXT520 (Vaisala), installed at T2 and T3 respectively. These included temperature, humidity, rain amount, wind speed, and wind direction. Instruments at both sites had similar resolution and accuracy of about (± 0.3 °C), (± 3–5%), (5% for daily accumulation) and (± 3° and 0.3–0.5 m s^{-1}), respectively. U30 Station was used to compare the wind measurements at T2 by the Weather Sensor Lufft, WS800-UMB installed at 15 m a.g.l.

2.2.2. Aerosol physical properties

Particle scattering coefficients at three wavelengths were measured using two models of integrating nephelometers: Ecotech Aurora (450, 525 and 635 nm) and TSI 3563 (450, 550 and 700 nm), respectively at T2 and T3. At the T3 site, the PM_{10} scattering measurements, provided by ARM, were available on 1-h average. These scattering values were linearly interpolated to every 30 min to compare with the rest of the dataset. Truncation errors related to nephelometer angular illumination function were compensated according to Müller et al. (2009; 2011a) and Anderson and Ogren (1998). A background (zero) calibration was performed daily, and spans checks in the beginning of each IOP.

Particle absorption coefficients and black carbon equivalent (BCe) concentrations were measured at the T2 site using an aethalometer (Magee Scientific, Model AE33) at seven wavelengths (370–880 nm). Aethalometer data were compensated for filter loading and multiple scattering effects according to Schmid et al. (2006) and Rizzo et al. (2011). AMAAP absorption photometer (Thermo Inc., Model 5012) (Petzold et al., 2005; Petzold and Schönlinner, 2004) was also used at T2 to measure BCe concentrations at 637 nm, converted to absorption coefficients assuming a mass absorption coefficient of 6.6 m^{2}g^{-1}. Measurements were taken every minute, and a 5% correction was applied to the data to account for an adjustment of wavelength (Müller et al., 2011b).

Submicrometer particle size distributions (10–490 nm) were measured using SMPS systems (Scanning Mobility Particle Sizer, TSI models 3081 or 3082, long DMA) coupled to butanol-based condensation particle counters (CPC, TSI, models 3010 and 3772). Both CPC models have a nominal size range from 10 nm to 3 μm and concentration range from 0 to 10^4 cm^{-3}, with a counting efficiency up to 90% for particles with 20 nm diameters. The aerosol particle concentrations (CN) are given by the integration of the size distribution between 10 and 490 nm.

2.2.3. Trace gases and aerosol chemical properties

Carbon monoxide and sulfur dioxide mixing ratios were monitored at both sites using the trace gas analyzers LGR N2O/CO-23D and Thermo 43i-TLE, respectively. The LGR-ICOS instrument was calibrated using a standard CO gas cylinder provided by National Oceanic Atmospheric Administration (NOAA). Background checks for SO_2 were conducted monthly using a bed of activated charcoal.

The chemical composition of submicrometer aerosols was measured on line by mass spectrometry using an Aerosol Chemical Speciation Monitor (ACSM) and a High-Resolution Time-of-Flight Aerosol Mass Spectrometer (HR-ToF-AMS), both from Aerodyne Research Inc.,

installed at the T2 and T3 sites, respectively. The aerosol mass spectrometers characterized in real-time (with resolution better than 15 min) a wide range of non-refractory sub-micron aerosol particles such as organics, nitrate, sulfate, ammonium, and chloride (Decarlo et al., 2006; Ng et al., 2011). At T2, the ACSM was operated continuously throughout the year of 2014 and calibrated monthly, whereas at T3 the HR-ToF-AMS was operated during the IOPs and calibrated every five days (De Sá et al., 2017). The calibration procedures were conducted using mono-disperse ammonium nitrate and ammonium sulfate particles generated with an atomizer and size-selected with a DMA (Canagaratna et al., 2007).

2.3. Characterizing Manaus emissions

To characterize Manaus emissions, we used chemical indicators of anthropogenic activity such as CO, BC, SO_2, CN, and f_{60} (the fraction of total OA measured at mass-to-charge ratio m/z 60, a marker ion of primary biomass burning organic aerosol - BBOA) (Cubison et al., 2011; Jolleys et al., 2012; Lee et al., 2016; Nielsen et al., 2017), all analyzed according to local wind direction at T2. The site was considered under the influence of Manaus plume when wind direction ranged from 15° to 120° and the wind speed was greater than 1.0 m s^{-1}. This selection restricted the dataset to predominant easterly air masses from 06 to 18 h local time and reduced sample space during the nighttime, when the winds were weak (Fig. S1). To distinguish air masses at T2 impacted by the Manaus urban plume, we have used as criteria (1) the prevailing winds from Manaus city (15–120°) and (2) a f_{60} threshold of 0.35% to exclude the effects of local fires emitted near the T2, especially those emitted by brick factories. In this study we tested the use of the enhancement ratios of BCe and CN to carbon monoxide enhancement to derive the Manaus plume chemical signature, but no statistically significant difference was found between normalized enhancement ratios observed from brick factories (prevailing winds from the south) and those from Manaus (prevailing winds from 15 to 120°), as shown in Figure S2. Although SO_2 was a clear indicator of the Manaus plume (not shown), it was not used because its concentration was not measured at T3. As a result of our analysis, we concluded that the wind direction from Manaus and $f_{60} < 0.35\%$ were the best metrics for identifying the Manaus plume at the T2 site. At T3, the influence of the Manaus plume was detected based on the f_{60} threshold (lower than 0.35%) observed at T2, taking into account the prevailing winds from Manaus, CN measurements above the background level at T0 and simulated back trajectories (as described in the next section). Clean air masses that eventually satisfied the proposed f_{60} range (< 0.35%) were removed by applying an aerosol number concentrations threshold. The lower bound for aerosol number concentrations at T3 to be considered as originating from Manaus was calculated weekly, based on the average aerosol concentration plus one standard deviation at T0a, located at a remote site upwind of Manaus. Using the proposed criteria, periods of influence of the Manaus urban plume at both sites (T2 and T3), with direct plume transport witihin the planetary boundary layer (PBL), and without influence of precipitation or local biomass burning emissions, were selected, comprising about 25% of the total observation period.

To study how the plume evolved from T2 to T3, we made use of enhancement ratios (Andreae and Merlet, 2001; Gouw and Jimenez, 2009; Akagi et al., 2011; Sahu et al., 2012; Jolleys et al., 2012). We use the normalized excess ratios given by ΔX/ΔCO (Sahu et al., 2012), where ΔX was the excess concentration of a given species and ΔCO was the enhancement of CO (a non-reactive smoke tracer), considering here a background value of 83 ppb, as observed during the clean periods of LBA-CLAIRE-2001 (Kuhn et al., 2010) and SMOCC (Andreae et al., 2004) experiments. Our baselines for CN and non-refractory species were determined from the observations of background conditions during the AMAZE-2008 experiment (Chen et al., 2015; S. T. Martin et al., 2010b).

2.4. Back-trajectories between T3 and T2 sites

The plume transport between the two sampling sites was modeled using back trajectory calculations. Back trajectories were used to associate pairs of measurements from the two sites as being different samples of the same air mass. Trajectories were calculated with the HYSPLIT model (Draxler, 2007; Stein et al., 2007). Meteorological fields from the Global Assimilation Data System (GDAS), provided by NOAA Air Resources Laboratory (ARL) as a regular grid/scale of 0.5° by 0.5° in space, 18 levels of pressure and 3 h interval in time, were used to drive the model. Back-trajectories were calculated arriving at 100 m above the T3 site for every 30 min during each IOP. For studying the urban plume evolution between T2 and T3, we selected only back-trajectories going over T2 (a 20 km × 20 km box), within the PBL (below 1000 m). To improve the confidence in this selection, only straight trajectories were considered, i.e., when meteorological conditions were such that winds were rather uniform. Lastly, we selected only trajectories having no precipitation along the transect during the IOPs (~25% of 5712 simulated

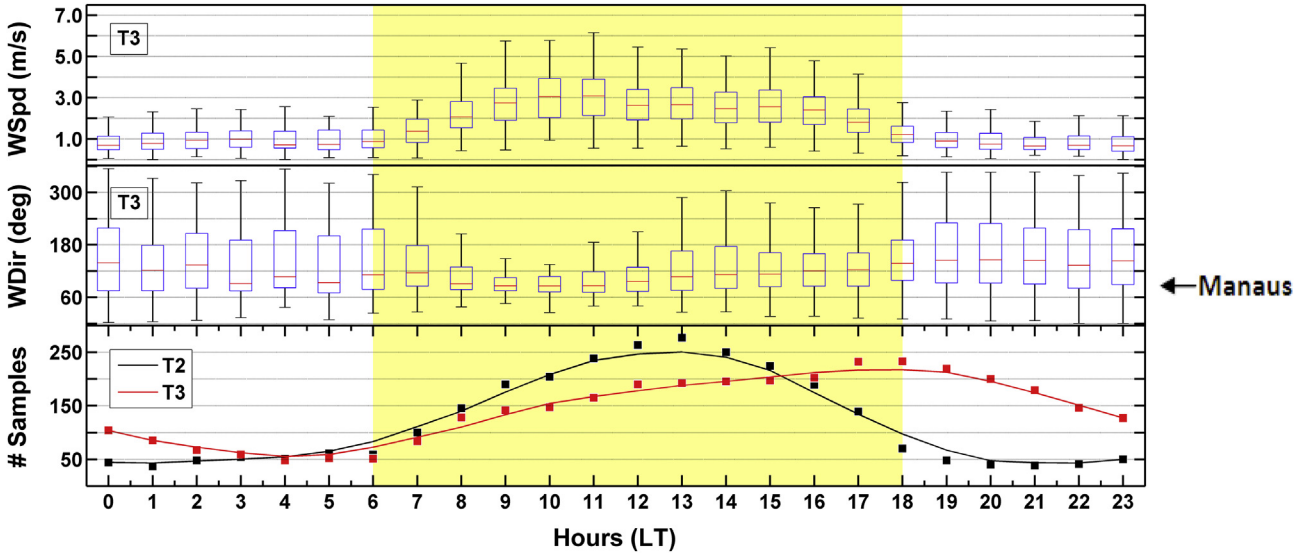

Fig. 2. Hourly box-plots of 30-min averaged wind speed (top) and direction (in middle) observed at the T3 site, for all data from 01/Feb/2014 to 15/Oct/2014, showing a prevalence of winds coming from the direction of Manaus with high wind speed during the daytime. The black vertical lines show the standard deviation for wind speed (top) and wind direction (in middle). The bottom panel shows the frequency of events in which air masses were apportioned to Manaus emissions at T2 (black, close to Manaus) and T3 (red, 70 km downwind Manaus), based on ΔCN/ΔCO. As back trajectories were not used as a constraint, the numbers of samples are different for the two sites. Local time (LT) is UTC-4 hours. Yellow coloring represents daylight hours. Detailed aspects of the wind prevailing in the directions of T2 and T3 are shown in Fig. S1 and S3, respectively. (For interpretation of the references to color in this figure legend, the reader is referred to the Web version of this article.)

cases), based on the CMORPH (CPC MORPHing technique) precipitation data at high spatial and temporal resolution (Joyce et al., 2004).

3. Results and discussion

3.1. Plume transport T2-T3

Fig. 2 shows the daily variation of wind direction and speed at ground level at T3. The lower panel shows the time of the day when the Manaus plume was identified at T2 and T3. The Manaus plume influence was more frequent at T3 during the daytime and started to decrease in the first night hours having a minimum before dawn. Out of the 5712 periods of 30 min along the IOPs 1 and 2, after applying the selection criteria to detect the influence of the Manaus plume at T3 (section 2.3 and 2.4), the sample space was reduced to 600 (22%) data points during IOP 1 (wet season) and 800 (29%) data points during IOP 2 (dry season), summing up to 1400 data points. The trajectories selected for the study of the plume evolution are shown in cyan (~1400 cases) in Fig. 3. The trajectory density with the coverage areas for all simulated back trajectories over sites is also shown (Figure S3). The transport time of selected air masses (no rain) from T2-T3 ranged from 3.5 to 5.5 h, having an average value of 4.6 (± 0.9)h and a median of about 4.5 h. This result is compatible with an average wind speed of 4.3 m s^{-1}. This is two times greater than mean values (of about 2.0 m s^{-1}) found by the anemometers at ~ 15 m of height above ground level at T2 and T3. However, it is in line with average wind speed values measured by SODAR at T3, at the 50 and 100 m above ground level, from February to December 2014 (Figure S3).

3.2. Chemical composition

The chemical composition of aerosols can provide information on the dominant sources and evolution of pollution in different plumes (Sahu et al., 2012). The enhancement ratios ΔCN/ΔCO, ΔOA/ΔCO, and inorganic aerosols, such as $\Delta SO_4/\Delta CO$, $\Delta NH_4/\Delta CO$ and $\Delta NO_3/\Delta CO$ are presented in Table 1. The changes in concentration for aerosol chemical species are presented in Table S2.

As expected, the average CN decreased along the trajectory T2-T3 as a result of dry deposition and probable coagulation of aerosol concentration by Brownian diffusion of small particles. Differences in the PBL height could be also considered as one possible reason for observed differences in the surface aerosol concentration between T2 and T3. However, previous results from Amaze-08 experiment (Baars, 2011) showed that aerosols are not confined to, and hence not modulated by, the PBL due to the constant and strong convective activity in the region, even during the dry season. The average ΔCN/ΔCO ratios observed during the wet and dry seasons were respectively 153 and 68 cm^{-3} ppb^{-1} at T2 and 107 and 47 cm^{-3} ppb^{-1} at T3, a reduction of 30% along the trajectory T2-T3 (Table 1). This reduction is consistent with decreasing of the ΔCN/ΔCO observed during the GoAmazon 2014/5 and LBA-CLAIRE-2001 experiment using aircraft measurements (Fig. S5). However, at the T2, the values are still 2–3 times lower than the 339 cm^{-3} ppb^{-1} found in the Manaus plumes during the LBA-CLAIRE-2001 flights (Kuhn et al., 2010). The change in the pattern of power generation in the Manaus city is a possible cause of this reduction (Medeiros et al., 2017).

Conversely, during the dry season the OA mass concentration increased by 30%, from 7.3 μg m^{-3} at T2 to 9.5 μg m^{-3} at T3, on average (Table S2). This increase can be directly attributed to secondary organic aerosol formation (Hallquist et al., 2009), and also could have a contribution from entrainment of air containing BBOA emitted along the trajectory T2-T3, since this increase was mostly observed in the dry season. This could also be partly a result of slower SOA formation during the wet season, when cloudier skies likely led to lower ambient oxidant concentrations and slower chemistry in the atmosphere (Andreae et al., 2015; Artaxo et al., 2013). OA mass enhancements were observed mainly throughout the light hours of the day (11:00–17:00, LT) and the beginning of the evening (18:00–20:00, LT). In central Amazonia, upwind of Manaus, the OA concentration was observed to range from 0.3 to 0.5 μg m^{-3} in the wet season, under background conditions (Andreae et al., 2015; Artaxo et al., 2013) to 2.1–6.3 μg m^{-3} in the dry season, under perturbed conditions by regional BBOA emissions (Andreae et al., 2015; Gabey et al., 2010; Whitehead et al., 2016a). The concentration range observed at T2 indicates a strong impact of Manaus emissions on atmospheric composition.

When normalized by ΔCO to account for dilution in the trajectory (Table 1), the average ratio ΔOA/ΔCO at T2 is about 46 μg m^{-3} ppm^{-1} in the wet season, and 86 μg m^{-3} ppm^{-1} in the dry season. These values can be compared to biomass burning emissions in western Amazonia, where a

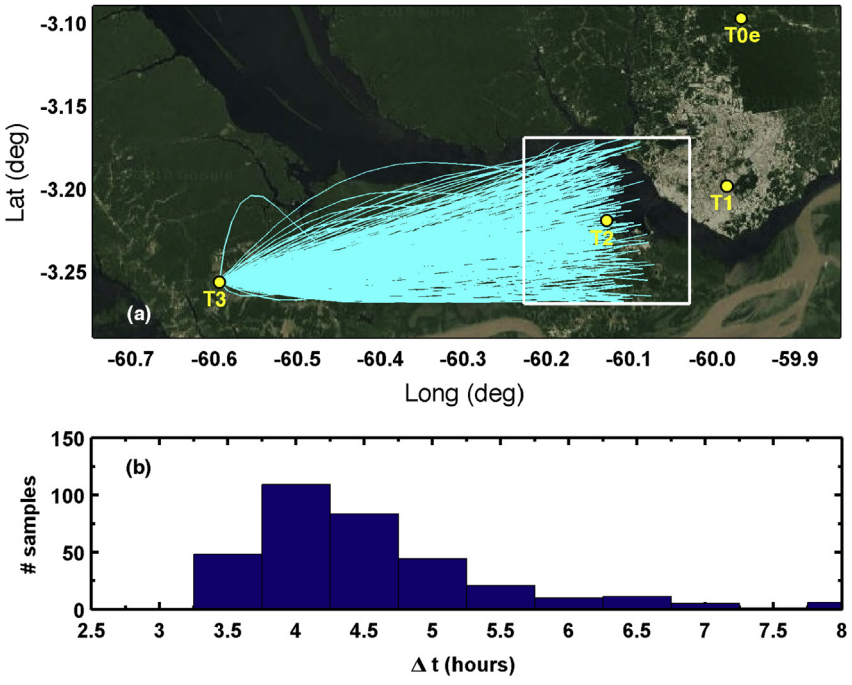

Fig. 3. Panel (a) shows the back trajectories calculated for studying the plume evolution. A subset of straight trajectories without precipitation, eastward from T3 (70 km downwind Manaus), inside the PBL (altitude < 1000 m) and reaching a 20 × 20 km box around T2 (close to Manaus) is represented in cyan. The trajectories were simulated as arriving at 100 m above T3. Panel (b) shows the histogram of air mass transport time between T2 and T3 based on the trajectories shown in cyan (a). (For interpretation of the references to color in this figure legend, the reader is referred to the Web version of this article.)

Table 1
Changes on particle number concentration (CN), CO mixing ratios and enhancement ratios of aerosol chemical components, resulting from evolution of the Manaus plume between the sampling sites (T2 and T3) during IOP 1 (1 February to 31 March 2014) and IOP 2 (15 September to 15 October 2014). Concentrations and enhancement ratios are shown at departure and arrival times of air masses leaving the T2 site and reaching the T3 site.

Chemical Species	Departure from T2		Arrival at T3		Relative Factor (T3/T2)	
–	IOP 1	IOP 2	IOP 1	IOP 2	IOP 1	IOP 2
CN - cm^{-3}						
Median	5599	5436	2832	3807	0.5	0.7
Average	5935	5806	3450	3949	0.6	0.7
Std. Deviation (±)	2237	2048	2381	1487	–	–
CO - ppb						
Median	130	159	119	165	0.9	1.0
Average	130	168	118	175	0.9	1.0
Std. Deviation (±)	24	33	11	49	–	–
$\Delta CN/\Delta CO$ - $cm^{-3}ppb^{-1}$						
Median	127	58	74	39	0.6	0.7
Average	153	68	107	47	0.7	0.7
Std. Deviation (±)	112	31	113	21	–	–
$\Delta OA/\Delta CO$ - $\mu gm^{-3}ppm^{-1}$						
Median	35	93	33	117	0.9	1.3
Average	46	86	47	119	1.0	1.4
Std. Deviation (±)	33	27	38	29	–	–
$\Delta SO_4/\Delta CO$ - $\mu gm^{-3}ppm^{-1}$						
Median	5.3	19.4	0.9	25.8	0.2	1.3
Average	6.6	18.3	2.3	22.9	0.3	1.3
Std. Deviation (±)	6.2	6.1	4.9	8.7	–	–
$\Delta NO_3/\Delta CO$ - $\mu gm^{-3}ppm^{-1}$						
Median	1.8	3.7	0.7	2.2	0.4	0.6
Average	2.6	3.7	0.9	2.3	0.3	0.6
Std. Deviation (±)	1.8	1.2	0.8	0.9	–	–
$\Delta NH_4/\Delta CO$ - $\mu gm^{-3}ppm^{-1}$						
Median	1.7	5.8	1.2	7.4	0.7	1.3
Average	2.2	5.8	1.7	7.0	0.8	1.2
Std. Deviation (±)	2.5	2.3	1.9	2.5	–	–

fairly constant ΔOA/ΔCO ratio of 30 $\mu g\,m^{-3}\,ppm^{-1}$ over a wide range of plume ages was observed (Brito et al., 2014). The values of ΔOA/ΔCO at T3 are similar to measurements of pollution outflow from urban regions after about 1 day of plume processing: Mexico City (73 $\mu g\,m^{-3}\,ppm^{-1}$ CO, Kleinman et al., 2008), eastern USA (103 $\mu g\,m^{-3}\,ppm^{-1}$ CO, Kleinman et al., 2007), southwestern USA (70 $\mu g\,m^{-3}\,ppm^{-1}$ CO, Weber et al., 2007), London (50 $\mu g\,m^{-3}\,ppm^{-1}$ CO, McMeeking et al., 2012), and Paris (100–130 $\mu g\,m^{-3}\,ppm^{-1}$ CO, Freney et al., 2014). Other reference values are also summarized in DeCarlo et al. (2010).

In the dry season, presumably due to contribution of biomass burning emissions, the summed submicron particle concentration (OA, SO_4, NH_4, and NO_3) was significantly higher than that of the wet season (Table S2). In both seasons, without taking into account the BCe mass, OA was the largest contributor (~80%), followed by sulfate (~13%), nitrate (~5%), and ammonium (1.5%). The average concentrations in the plume of the non-refractory aerosols SO_4, NO_3 and NH_4 were 0.30, 0.10 and 0.10 $\mu g\,m^{-3}$ in the rainy season and 1.9, 0.25, and 0.50 $\mu g\,m^{-3}$ in the dry season, respectively. During the plume evolution in the T2-T3 path there was an increase of 25% and 20% in the enhancement ratios of $\Delta SO_4/\Delta CO$ and $\Delta NH_4/\Delta CO$, mainly in the daytime between 11 and 18 h (LT) (Table 1). The increase on SO_4 can be attributed to secondary inorganic aerosol formation, especially due to the SO_2 oxidation during the transect (Luria et al., 2001; Dunlea et al., 2009; Kang et al., 2011; Kagawa and Ishizaka, 2014). Changes in the $\Delta SO_4/\Delta CO$ ratio for anthropogenic pollution plumes are also associated with the time scale of oxidation of sulfate versus SOA precursors, which first increase as SOA forms, and then decrease as sulfate forms on a longer time scale (Brock et al., 2008, 2011; Dunlea et al., 2009; Kang et al., 2011; Kondo et al., 2011). Conversion rates (gas-phase) SO_2-to-SO_4 can be enhanced due to greater availability of OH radicals in the atmosphere during the dry season, when the concentrations of NO_x are usually larger, increasing the potential for SO_4 formation. In the wet season, following an opposite trend compared to the dry season, there was a decrease in the average enhancement ratios of aerosol chemical components, especially $\Delta SO_4/\Delta CO$ and $\Delta NO_3/\Delta CO$. The $\Delta SO_4/\Delta CO$ reduction verified during the plume evolution in the wet season can be associated with dry deposition and scavenging by cloud droplets. In addition, during the wet season, there may not be sufficient amounts of OH radicals to allow the sulfur dioxide to be converted to sulfate completely (Hallquist et al., 2009; Kang et al., 2011). Furthermore, the availability of H_2O_2 in clouds during the year may be controlling the rates of conversion to SO_2 or SO_4 by unknown nonlinear mechanisms. In this study, the conversion rate SO_2-to-SO_4 could not be calculated as there were no SO_2 measurements at the T3 site. Concerning to the $\Delta NO_3/\Delta CO$ ratio, there was a sharp decrease of about 30–60% during the urban plume transport in both seasons. The possible mechanisms affecting the formation processes of O_3 and OH during the evolution of the plume, in conjunction with the high urban NO_y emissions, may explain the changes in the dominant daytime nitrate production pathway (NO_2 + OH). The decrease of $\Delta NO_3/\Delta CO$ can be possibly also associated with the reduction of VOCs and O_3 concentrations during the plume evolution, since most organonitrates in the atmosphere are produced either by oxidation reactions of biogenic VOCs (e.g., isoprene), and photochemical mechanisms (e.g., OH radicals), processes which are affected by cloud cover (DeCarlo et al., 2008; Farmer et al., 2010; Szmigielski, 2013).

3.3. Aerosol size distribution

The average aerosol number size distributions observed at T2 and T3 are shown in Fig. 4 for IOP 1 (wet season) and IOP 2 (dry season) considering periods of influence of the Manaus plume. During IOP 1, the median particle size distribution observed at T2 shows a prominence of ultrafine and Aitken modes, respectively centered at 20 and 55 nm. This observation is attributed to the primary particulate emissions from industries, power plants, transportation, natural sources, and secondary material condensed on the Aitken nuclei (10–100 nm), given the proximity to Manaus city. Particle number concentration at T2 is higher than at T3, and observations at T3 indicate a substantial decrease in number concentration over the entire size range. Fig. 4

also suggests particle growth along the transport from T2 to T3, showing a shift in the nucleation mode from around 20 nm–35 nm, and in the Aitken mode, from ca. 55 nm–65 nm. Under rainless conditions, both coagulation and condensation could cause this apparent particle growth. The overall decrease in number concentration, and also in mass during the wet season, is somewhat surprising as no major sinks of aerosol mass except wet deposition is likely to cause such a large reduction in number and mass during the timescale of transport between the two sites. However, there are other possible explanations: it is likely that the precipitation data derived from the CMORPH technique is not accurate enough for this study, and that we in fact do have precipitation or fog events in many of the cases of transport between T2 and T3 during IOP 1 in spite of the filtering. The effect of dilution of the plume into surrounding 'clean' air masses may also have contributed to the decreasing in the total concentrations of particles since the size distribution was not normalized by enhancement of CO (although that is not enough, as ΔCO varies from 47 to 35 ppb (74%) from T2 to T3 during IOP 1). Another explanation might be an enhanced dilution effect due to the strong deep convection during the wet season (strong convergence of humidity, high vertical motion, and latent heat release).

During periods under the influence of the Manaus plume in the IOP 2, the median particle number size distribution at T2 is also dominated by the ultrafine and Aitken modes, respectively centered at 30 nm and 60 nm. Similar to IOP 1, a decrease on particle number concentration and an increase on particle size were observed from T2 to T3. The number concentration of particles between 90 and 200 nm is substantially higher at T3 than at T2, suggesting a rather pronounced condensation growth, given the short transport time. Supporting the hypothesis of particle growth by condensation, the ratios ΔOA/ΔCO and $\Delta SO_4/\Delta CO$ suggest an enhancement of OA and SO_4 during the transport. This could have its origin in both photochemical ageing of the plume (e.g. transformation of SO_2 to SO_4^{2-} and oxidation of various anthropogenic organic compounds) and condensational growth, but it could also suggest the contribution of aged biomass burning emissions, leading to the observed increase on the concentration of particles in the 90–200 nm size range. As particles in this size range can easily act as cloud condensation nuclei (Kuhn et al., 2010), they are likely of relevance for the radiative budget over the region. It is also apparent that the number of particles > 200 nm is lower at T3 as compared to T2, which might be indicative of dry deposition. In order to gain more insight in what processes govern the size distribution evolution we have also simulated the evolution of the average aerosol number size distribution observed at T2 under different conditions, using a simplified setup of the CALM model (Tunved et al., 2010). The modeling effort, which was iterative by nature, evaluated a number of different assumptions regarding source generation rate of condensable gases, nucleation rate and dilution during the on average 4.5 h of transport between the two sites. The simulations were all initialized with the observed size distribution at T2 (Fig 6) and the results were compared with the average of the observed number size distribution at T3. During all simulated cases, we assumed activation type nucleation (Kulmala et al., 2006), i.e. the nucleation rate is directly proportional to the sulfuric acid concentration as $J_1 = A\ [H_2SO_4]$, where J_1 represents the nucleation rate and A represents the activation coefficient, which is an environmental dependent parameter. A reasonable combination of parameters that provided numerical agreement between observed and simulated aerosol size distribution at T3 using these simplified assumptions was an activation coefficient A of $5*10^{-7}$, a source rate of H_2SO_4 of $1*10^6\ cm^{-3}s^{-1}$ and a source rate of condensable organic gases of $1*10^6\ cm^{-3}s^{-1}$ (assuming Mw_{org} of 186 g mol^{-1} and saturation vapor pressure of $3*10^{10}\ m^{-3}$).

As shown in Fig. 5, Frame A, it is clear that the number concentration in the accumulation mode size range is substantially overestimated by the model. Thus, it was found that in order to support the growth of the aerosol into the accumulation mode, but without getting to big disagreement in number between observed and modeled size distribution at T3, dilution was necessary. Thus, in the final simulation we assumed a dilution factor of the plume of 0.95 h^{-1} which gave reasonable results together with the abovementioned source rates of condensable gases (Fig. 5, Frame B). From the simulations it was further evident that nucleation was indeed needed to support the evolution of the size distribution in order to resemble the observed features, as shown in Fig. 5, Frame C, showing a simulation as above, but with nucleation disabled. Thus, the observed features during IOP 2 are at least qualitatively, and to some degree quantitatively, consistent with aerosol ageing due to mainly coagulation, condensation and dry deposition in the absence of clouds and rain.

Certainly, crude simulations like this by nature are very uncertain, but the result at least suggests that with reasonable source strengths of condensable and nucleating gases, we are able to simulate the evolution of the aerosol during the transport between T2 and T3. More detailed analysis and simulations are encouraged in order to better understand the governing processes during transport of this polluted plume over the rain forest.

3.4. Aerosol optical properties

The main changes in the aerosol optical properties are shown in Table 2. We have used the single scattering albedo (SSA) as an indicator of the direct radiative effect of the particles in the atmosphere, since it is considered a key parameter in determining the direct effect of aerosol particles on climate as well as to get information regarding particle composition (Bergstrom et al.,

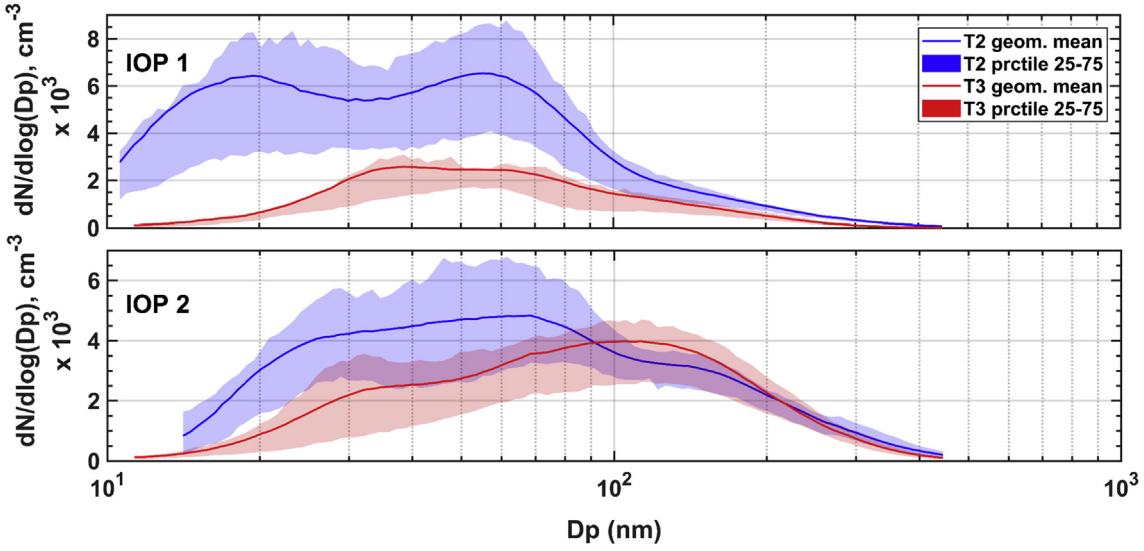

Fig. 4. Mean particle number size distribution at T2 (blue line, close to Manaus) and T3 (red line, 70 km downwind Manaus) for the wet (IOP 1, top) and dry (IOP 2, bottom) seasons, considering selected periods under the influence of the Manaus urban plume. The blue and red shaded areas show 25–75 percentiles at T2 and T3 sites, respectively. (For interpretation of the references to color in this figure legend, the reader is referred to the Web version of this article.)

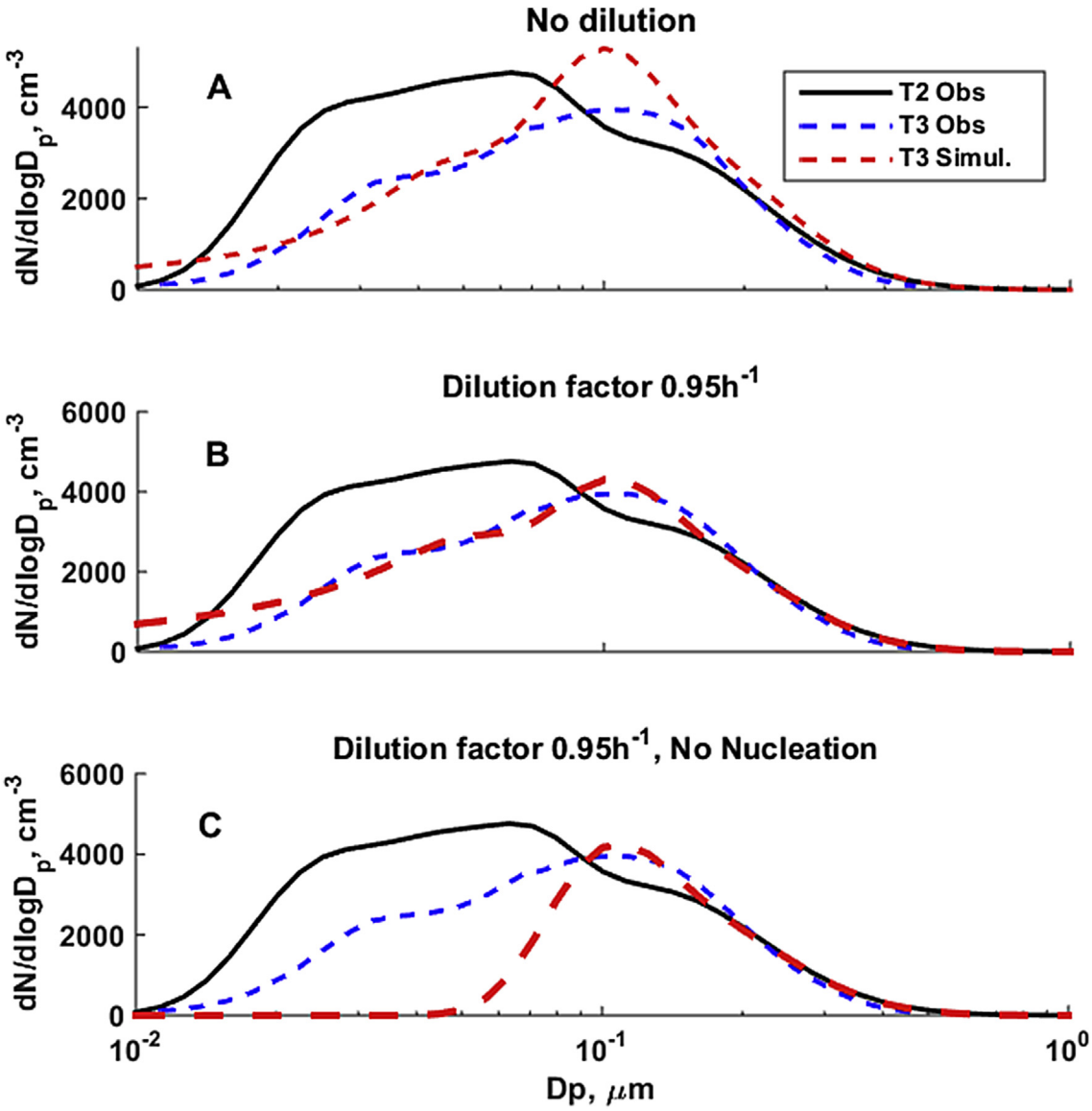

Fig. 5. Result of simplified aerosol dynamic simulation during 4.5 h using the fit of the average number size distribution at station T2 (close to Manaus) as input aerosol (solid black) with observed size distribution at T3 (70 km downwind Manaus) in blue and simulated result at T3 in dashed red. Frame A shows simulation without dilution, but with nucleation enabled. Frame B shows simulation assuming a dilution factor of 0.95 h^{-1} and frame C shows simulation as above, but with nucleation disabled. (For interpretation of the references to color in this figure legend, the reader is referred to the Web version of this article.)

2010, 2002; Dubovik and King, 2000; Lim et al., 2014; Russell et al., 2010; Takemura et al., 2002, 2000). Due to biomass burning in the Amazon basin in the dry season, there was an about fourfold increase of particle scattering and absorption coefficients relative to the wet season and an increase of about 10% on the SSA at 450–700 nm at both sites (T2 and T3). Particle scattering and absorption coefficients decreased by 20–25% and 40–50% from T2 to T3, respectively (Table 2). This decrease was mainly attributed to the pollution dilution effect between sites, (Kleinman et al., 2008). On average, the scattering ranged from 9.9 to 6.6 Mm^{-1} and 51.0 to 29.1 Mm^{-1} between sites, while absorption decreased from 6.8 to 1.9 Mm^{-1} and 9.6 to 4.6 Mm^{-1} in the transect in the wet and dry seasons, respectively. However, when the particle scattering coefficients are normalized by CN, an increase of up to 50% was observed in the wet season, whereas in the dry season a slight reduction of about 10% was observed (Table 2). These scattering values, as well as SCAT/CN, are compatible with previous measurements in the Manaus area (Kuhn et al., 2010; Trebs et al., 2012) and consistently higher than the scattering values reported by Rizzo et al. (2013) in the south of the Amazon during the wet season. It may also be the result of rapid deposition of larger particles than the 500 nm cutoff not monitored by the SMPS systems. These particles could likely have a great impact on the SSA. As discussed under section 3.1.2, deposition gets increasingly important for larger sizes, e.g. dust and other mechanically generated particles expected to be present in the urban environment.

For the outflow of the Manaus urban plume at T2, the values for SSA 0.60 and 0.80 in the wet and dry seasons, respectively, indicated the presence of a relatively large fraction of absorbing material. However, an average increase in the SSA of about 20% was observed during the Manaus plume evolution from T2 to T3, which can be directly associated with the formation of efficiently scattering SOA aerosols in the transect. During evolution of the plume the SSA average values ranged from 0.60 to 0.80 and 0.80 to 0.90 during the wet and dry seasons, respectively. These numbers are statistically equivalent to those reported for urban areas under conditions similar to this study, such as Atlanta, USA, of about 0.84 (Carrico, 2003), Ahmedabad, western India, of 0.88 (Ramachandran and Rajesh, 2007), Beijing, China, of about 0.80 (He et al., 2009), Mexico City of 0.75 (Eidels-Dubovoi, 2002; Kalafut-Pettibone et al., 2011), São Paulo, Brazil, 0.76 (Backman et al., 2012), and Granada, Spain, of 0.55–0.60 (Lyamani et al., 2010). In addition, we also observed an average increase of 15 and 50% in the scattering Angström exponent (SAE) from wet to dry season at both sites, as well as during the plume evolution. The SAE is an intensive

Table 2
Changes in aerosol optical properties resulting from evolution of the Manaus plume between sampling sites (T2 and T3) during the IOP 1 (1 February to 31 March 2014) and IOP 2 (15 September to 15 October 2014): particle scattering coefficient at 637 nm (SCAT), particle absorption coefficient at 637 nm (ABS), single scattering albedo at 637 nm (SSA) and scattering Angström exponent in the range 450–700 nm (SAE). Optical properties and enhancement ratios are shown at departure and arrival times of air masses leaving the T2 site and reaching the T3 site.

Optical Properties	Departure from T2		Arrival at T3		Relative Factor (T3/T2)	
–	IOP 1	IOP 2	IOP 1	IOP 2	IOP 1	IOP 2
SCAT (Mm^{-1})						
Median	9.2	53.8	6.8	31.1	0.8	0.6
Average	9.9	51.0	6.6	29.1	0.7	0.6
Std. Deviation (±)	4.1	25.8	2.1	12.2	–	–
SCAT/CN ($Mm^{-1}cm^{-3}$)						
Median	1.6	8.6	2.6	7.0	1.7	0.8
Average	1.8	9.9	2.7	8.4	1.5	0.9
Std. Deviation (±)	1.2	5.6	0.9	4.9	–	–
ABS (Mm^{-1})						
Median	5.8	8.8	1.8	4.7	0.3	0.5
Average	6.8	9.6	1.9	4.6	0.3	0.5
Std. Deviation (±)	4.0	4.8	1.4	1.7	–	–
ABS/ΔCO ($Mm^{-1}ppb^{-1}$)						
Median	0.1	0.1	0.0	0.1	0.3	0.6
Average	0.2	0.1	0.1	0.1	0.4	0.5
Std. Deviation (±)	0.1	0.1	0.0	0.0	–	–
SSA						
Median	0.6	0.8	0.8	0.9	1.3	1.1
Average	0.6	0.8	0.8	0.9	1.3	1.1
Std. Deviation (±)	0.1	0.1	0.1	0.0	–	–
SAE						
Median	1.4	1.6	1.6	2.4	1.1	1.5
Average	1.4	1.6	1.6	2.4	1.1	1.5
Std. Deviation (±)	0.3	0.3	0.4	0.2	–	–

parameter and is expected to decrease as the particle diameter increases (Lim et al., 2014; Rizzo et al., 2013; Russell et al., 2010; Schuster et al., 2006). The SAE also increased from wet to dry season at both sites, in accordance with the input of fine mode particles from biomass burning emissions. On average, under conditions of air polluted by Manaus, our results show SAE of 1.43 and 1.59 at T2 in the outflow of the Manaus urban plume, and 1.70 to 2.30 downwind at T3 during the wet and dry seasons, respectively. This observation is consistent with the absorption Angström exponent (AAE) values for these periods of 1.40 and 1.50 for T2 and T3, respectively. These results suggest a mixing of fine particles with other particles containing a fraction of absorbing material. Local emissions from biomass burning plumes may not have been completely excluded by the methods of this study. Overall, these results are supported by measurements of particle size distribution, which show an evolution in the average particles size from 20-40 nm to 100 nm in the transport between T2 and T3. The causes of the changes observed in the optical properties during the transport to T3 could include a multiplicity of non-linear processes, including secondary organic formation and inorganic aerosol particles, with direct effects on the chemical and physical properties of particles. Another important point here is that the studied optical properties refer to dry aerosols so that if the radiative forcing is calculated from the reported optical properties it may be underestimated. However, since aerosols have a low hygroscopicity in the Amazon (Rissler et al., 2006; Thalman et al., 2017; Whitehead et al., 2016b; Zhou et al., 2002), a small effect is expected for the radiative forcing.

4. Conclusions

Ground-based observations of aerosol chemical and optical properties from an urban site, Manaus, in the central Amazon region were investigated during the intensive operating periods of the GoAmazon 2014/5 experiment. CN, BC, CO and SO_2 concentrations, and absorption and scattering coefficients were analyzed to aid the characterization of the Manaus urban aerosol. These variables at T2 had a close dependence on the local wind, which was shown to be useful in identifying the Manaus plume at T2. In general, there was a wide variation in the gas and particle concentrations throughout the day, mainly associated with changes in the wind direction and, hence, changes in the air mass source within the Manaus urban area. High concentrations of CN and BC, often above 4500 particles cm^{-3} and 1000 ng m^{-3} respectively were observed at T2, located 8 km from the edge of Manaus. The dry air mole fraction of CO under the direct effect of Manaus pollution, mainly originating from power plants and motor vehicle emissions, was on average 145 ppb. In addition to the changes in the chemical composition of the natural aerosol of the pristine forest, optical properties were also impacted, with potential effects on the ecosystem, as e.g reducing of photosynthetic rates of the forest and its potential for carbon uptake. At T2, particle absorption and scattering coefficients increased by multiplicative factors 3.0 and 1.8 with respect to the near-pristine forest conditions (e.g. T0z, AMAZE-2008 experiment), respectively. The SSA, a key parameter in determining the climatic effects of aerosols, is about 10% lower compared to the near-pristine forest conditions, reaching values as low as 0.72 under the direct influence of the urban emissions, indicating a large fraction of absorbing material present in the Manaus plume, with a potential warming of the local atmosphere.

The combination of air masses from back trajectories simulated and chemical tracer as f_{60} was considered a satisfactory and practical method for analyzing the physical and chemical changes in the evolution of the aerosol plume during transport. This method identified a statistically acceptable percentage of cases in which T2 and T3 were under the direct influence of emissions from Manaus. The average time to transport the pollution between sites was estimated at 4.5 h. Overall, there was a reduction of trace gas and particle concentrations during transport, mainly attributed to the dilution effect of the plume with the cleaner air masses. Average decreases of about 6–8% in the CO concentrations and of about 10–25% in the particle concentrations were observed between the wet and dry seasons. Wet and dry removal processes, including coagulation, can reduce the concentration of particles along the transect.

An increase of 40% in the mass concentration of organic aerosols attributed to the formation of secondary organic aerosol during transportation was found in the dry season. There was a shift in the distribution of

particle size of 40–100 nm. Greater particle sizes were observed at the T3 site, possibly related to the production of secondary organic aerosol (SOA) and condensation of inorganic materials and organic oxidation products. The average increase of 30% in SO_4 concentrations during the dry season was attributed to the formation of inorganic aerosols, especially due to the SO_2 oxidation during transport. In the wet season, there was a decrease of up to 70% in the SO_4 concentrations compared to the wet season.

The observed changes in the characteristics of the population of aerosols downwind of the city (size distribution, quantity, and chemical composition) may be changing important properties of clouds, such as albedo and precipitation, thus contributing to impacts on the hydrological cycle and changes in radiative transfer rates, with still unknown indirect consequences for photosynthesis rates.

Acknowledgements

We thank FAPESP project 2013/05014-0 and 2013/50510-5 for financial support. We also thank financial support from CAPES and CNPq thought the projects 2013/457843-6 and 312131/2014-3. We acknowledge support from the Atmospheric Radiation Measurement (ARM) Climate Research Facility, a user facility of the United States Department of Energy (DOE), Office of Science, sponsored by the Office of Biological and Environmental Research, and support from the Atmospheric System Research (ASR) program of that office. We are also thankful for the support from UK Royal Society grant NA140450. We thank FAPEAM project 062.00568/2014. We acknowledge the National Institute for Amazonia Research (INPA) LBA Central Office for logistical support, and LBA Micrometeorology Lab, especially, Antônio Manzi, Alessandro C. de Araujo, Marta Sá, Leila Leal, Paulo Teixeira and Leonardo R. de Oliveira for all the support (maintenance and processing of K34 data). We thank several key persons for support on aerosol sampling and analysis: Simone R. Silva, Bruno T. Portela, Ana Lucia Loureiro, Fernando G. Morais, Fábio O. Jorge, Alcides C. Ribeiro, Juarez Viegas and Vagner Castro. We thank David Adams (UNAM) for his comments on the manuscript. The GoAmazon 2014/5 Experiment was conducted in part under scientific license 001030/2012–4 of the Brazilian National Council for Scientific and Technological Development (CNPq). BBP acknowledges support from a US EPA STAR Graduate Fellowship (FP-91761701-0). BBP and JLJ were partially supported by DOE DE-SC0016559.

Appendix A. Supplementary data

Supplementary data related to this article can be found at https://doi.org/10.1016/j.atmosenv.2018.08.031.

References

Akagi, S.K., Yokelson, R.J., Wiedinmyer, C., Alvarado, M.J., Reid, J.S., Karl, T., Crounse, J.D., Wennberg, P.O., 2011. Emission factors for open and domestic biomass burning for use in atmospheric models. Atmos. Chem. Phys. 11, 4039–4072. https://doi.org/10.5194/acp-11-4039-2011.

Anderson, T.L., Ogren, J. a., 1998. Determining aerosol radiative properties using the TSI 3563 integrating nephelometer. Aerosol Sci. Technol. 29, 57–69. https://doi.org/10.1080/02786829808965551.

Andreae, M.O., Acevedo, O.C., Araùjo, A., Artaxo, P., Barbosa, C.G.G., Barbosa, H.M.J., Brito, J., Carbone, S., Chi, X., Cintra, B.B.L., da Silva, N.F., Dias, N.L., Dias-Júnior, C.Q., Ditas, F., Ditz, R., Godoi, A.F.L., Godoi, R.H.M., Heimann, M., Hoffmann, T., Kesselmeier, J., Könemann, T., Krüger, M.L., Lavric, J.V., Manzi, A.O., Lopes, A.P., Martins, D.L., Mikhailov, E.F., Moran-Zuloaga, D., Nelson, B.W., Nölscher, A.C., Santos Nogueira, D., Piedade, M.T.F., Pöhlker, C., Pöschl, U., Quesada, C.A., Rizzo, L.V., Ro, C.-U., Ruckteschler, N., Sá, L.D.A., de Oliveira Sá, M., Sales, C.B., dos Santos, R.M.N., Saturno, J., Schöngart, J., Sörgel, M., de Souza, C.M., de Souza, R.A.F., Su, H., Targhetta, N., Tóta, J., Trebs, I., Trumbore, S., van Eijck, A., Walter, D., Wang, Z., Weber, B., Williams, J., Winderlich, J., Wittmann, F., Wolff, S., Yáñez-Serrano, A.M., 2015. The Amazon Tall Tower Observatory (ATTO): overview of pilot measurements on ecosystem ecology, meteorology, trace gases, and aerosols. Atmos. Chem. Phys. 15, 10723–10776. https://doi.org/10.5194/acp-15-10723-2015.

Andreae, M.O., Merlet, P., 2001. Emission of trace gases and aerosols from biomass burning. Global Biogeochem. Cycles 15, 955–966. https://doi.org/10.1029/2000GB001382.

Andreae, M.O., Rosenfeld, D., Artaxo, P., Costa, a a, Frank, G.P., Longo, K.M., Silva-Dias, M.A.F., 2004. Smoking rain clouds over the Amazon. Science 303, 1337–1342. https://doi.org/10.1126/science.1092779.

Artaxo, P., Rizzo, L.V., Brito, J.F., Barbosa, H.M.J., Arana, A., Sena, E.T., Cirino, G.G., Bastos, W., Martin, S.T., Andreae, M.O., 2013. Atmospheric aerosols in Amazonia and land use change: from natural biogenic to biomass burning conditions. Faraday Discuss 165, 203–235. https://doi.org/10.1039/C3FD00052D.

Baars, H., 2011. Aerosol Profiling with Lidar in the Amazon Basin during the Wet and Dry Season 2008. PhD thesis. Universitat Leipzig, Leipzig, pp. 191.

Backman, J., Rizzo, L.V., Hakala, J., Nieminen, T., Manninen, H.E., Morais, F., Aalto, P.P., Siivola, E., Carbone, S., Hillamo, R., Artaxo, P., Virkkula, A., Petäjä, T., Kulmala, M., 2012. On the diurnal cycle of urban aerosols, black carbon and the occurrence of new particle formation events in springtime São Paulo, Brazil. Atmos. Chem. Phys. 12, 11733–11751. https://doi.org/10.5194/acp-12-11733-2012.

Bergstrom, R.W., Russell, P.B., Hignett, P., Bergstrom, R.W., Russell, P.B., Hignett, P., 2002. Wavelength dependence of the absorption of black carbon particles: predictions and results from the TARFOX experiment and implications for the aerosol single scattering albedo. J. Atmos. Sci. 59, 567–577. < 0567:WDOTAO > 2.0.CO;2. https://doi.org/10.1175/1520-0469(2002)059.

Bergstrom, R.W., Schmidt, K.S., Coddington, O., Pilewskie, P., Guan, H., Livingston, J.M., Redemann, J., Russell, P.B., 2010. Aerosol spectral absorption in the Mexico City area: results from airborne measurements during MILAGRO/INTEX B. Atmos. Chem. Phys. 10, 6333–6343. https://doi.org/10.5194/acp-10-6333-2010.

Brito, J., Rizzo, L.V., Morgan, W.T., Coe, H., Johnson, B., Haywood, J., Longo, K., Freitas, S., Andreae, M.O., Artaxo, P., 2014. Ground-based aerosol characterization during the south american biomass burning analysis (SAMBBA) field experiment. Atmos. Chem. Phys. 14, 12069–12083. https://doi.org/10.5194/acp-14-12069-2014.

Brock, C. a., Sullivan, A.P., Peltier, R.E., Weber, R.J., Wollny, a., de Gouw, J.A., Middlebrook, a. M., Atlas, E.L., Stohl, A., Trainer, M.K., Cooper, O.R., Fehsenfeld, F.C., Frost, G.J., Holloway, J.S., Hübler, G., Neuman, J. a., Ryerson, T.B., Warneke, C., Wilson, J.C., 2008. Sources of particulate matter in the northeastern United States in summer: 2. Evolution of chemical and microphysical properties. J. Geophys. Res. Atmos. 113, D08302. https://doi.org/10.1029/2007JD009241.

Brock, C.A., Cozic, J., Bahreini, R., Froyd, K.D., Middlebrook, A.M., McComiskey, A., Brioude, J., Cooper, O.R., Stohl, A., Aikin, K.C., de Gouw, J.A., Fahey, D.W., Ferrare, R.A., Gao, R.-S., Gore, W., Holloway, J.S., Hübler, G., Jefferson, A., Lack, D.A., Lance, S., Moore, R.H., Murphy, D.M., Nenes, A., Novelli, P.C., Nowak, J.B., Ogren, J.A., Peischl, J., Pierce, R.B., Pilewskie, P., Quinn, P.K., Ryerson, T.B., Schmidt, K.S., Schwarz, J.P., Sodemann, H., Spackman, J.R., Stark, H., Thomson, D.S., Thornberry, T., Veres, P., Watts, L.A., Warneke, C., Wollny, A.G., 2011. Characteristics, sources, and transport of aerosols measured in spring 2008 during the aerosol, radiation, and cloud processes affecting Arctic Climate (ARCPAC) project. Atmos. Chem. Phys. 11, 2423–2453. https://doi.org/10.5194/acp-11-2423-2011.

Canagaratna, M.R., Jayne, J.T., Jimenez, J.L., Allan, J.D., Alfarra, M.R., Zhang, Q., Onasch, T.B., Drewnick, F., Coe, H., Middlebrook, A., Delia, A., Williams, L.R., Trimborn, A.M., Northway, M.J., DeCarlo, P.F., Kolb, C.E., Davidovits, P., Worsnop, D.R., 2007. Chemical and microphysical characterization of ambient aerosols with the aerodyne aerosol mass spectrometer. Mass Spectrom. Rev. 26 (2), 85–222. https://doi.org/10.1002/mas.20115.

Carrico, C.M., 2003. Urban aerosol radiative properties: measurements during the 1999 Atlanta supersite experiment. J. Geophys. Res. 108, 1–17. https://doi.org/10.1029/2001JD001222.

Cecchini, M.A., Machado, L.A.T., Comstock, J.M., Mei, F., Wang, J., Fan, J., Tomlinson, J.M., Schmid, B., Albrecht, R., Martin, S.T., Artaxo, P., 2016. Impacts of the Manaus pollution plume on the microphysical properties of Amazonian warm-phase clouds in the wet season. Atmos. Chem. Phys. 16, 7029–7041. https://doi.org/10.5194/acp-16-7029-2016.

Cecchini, M.A., Machado, L.A.T., Andreae, M.O., Martin, S.T., Albrecht, R.I., Artaxo, P., Barbosa, H.M.J., Borrmann, S., Fütterer, D., Jurkat, T., Mahnke, C., Minikin, A., Molleker, S., Pöhlker, M.L., Pöschl, U., Rosenfeld, D., Voigt, C., Wenzierl, B., Wendisch, M., 2017. Sensitivities of Amazonian clouds to aerosols and updraft speed. Atmos. Chem. Phys. Discuss. 10037–10050. https://doi.org/10.5194/acp-2017-89.

Chen, Q., Farmer, D.K., Rizzo, L.V., Pauliquevis, T., Kuwata, M., Karl, T.G., Guenther, A., Allan, J.D., Coe, H., Andreae, M.O., Pöschl, U., Jimenez, J.L., Artaxo, P., Martin, S.T., 2015. Submicron particle mass concentrations and sources in the Amazonian wet season (AMAZE-08). Atmos. Chem. Phys. 15, 3687–3701. https://doi.org/10.5194/acp-15-3687-2015.

China, S., Wang, B., Weis, J., Rizzo, L., Brito, J., Cirino, G.G., Kovarik, L., Artaxo, P., Gilles, M.K., Laskin, A., 2016. Rupturing of biological spores as a source of secondary particles in Amazonia. Environ. Sci. Technol. 50, 12179–12186. https://doi.org/10.1021/acs.est.6b02896.

Cirino, G.G., Souza, R.A.F., Adams, D.K., Artaxo, P., 2014. The effect of atmospheric aerosol particles and clouds on net ecosystem exchange in the Amazon. Atmos. Chem. Phys. 14, 6523–6543. https://doi.org/10.5194/acp-14-6523-2014.

Collow, A.B.M., Miller, M.A., Trabachino, L.C., 2016. Cloudiness over the amazon rainforest: meteorology and thermodynamics. J. Geophys. Res. 121, 7990–8005. https://doi.org/10.1002/2016JD024848.

Cubison, M.J., Ortega, A.M., Hayes, P.L., Farmer, D.K., Day, D., Lechner, M.J., Brune, W.H., Apel, E., Diskin, G.S., Fisher, J.A., Fuelberg, H.E., Hecobian, A., Knapp, D.J., Mikoviny, T., Riemer, D., Sachse, G.W., Sessions, W., Weber, R.J., Weinheimer, A.J., Wisthaler, A., Jimenez, J.L., 2011. Effects of aging on organic aerosol from open biomass burning smoke in aircraft and laboratory studies. Atmos. Chem. Phys. 11, 12049–12064. https://doi.org/10.5194/acp-11-12049-2011.

Da Rocha, H.R., Manzi, A.O., Cabral, O.M., Miller, S.D., Goulden, M.L., Saleska, S.R., Coupe, N.R., Wofsy, S.C., Borma, L.S., Artaxo, R., Vourlitis, G., Nogueira, J.S., Cardoso, F.L., Nobre, A.D., Kruijt, B., Freitas, H.C., Von Randow, C., Aguiar, R.G., Maia, J.F., 2009. Patterns of water and heat flux across a biome gradient from tropical forest to savanna in Brazil. J. Geophys. Res. Biogeosciences 114, 1–8. https://doi.org/10.1029/2007JG000640.

Davidson, E.A., de Araújo, A.C., Artaxo, P., Balch, J.K., Brown, I.F., Bustamante, M.M.C.,

Coe, M.T., DeFries, R.S., Keller, M., Longo, M., Munger, J.W., Schroeder, W., Soares-Filho, B.S., Souza, C.M., Wofsy, S.C., 2012. The Amazon basin in transition. Nature 481, 321–328. https://doi.org/10.1038/nature10717.

De Sá, S.S., Palm, B.B., Campuzano-Jost, P., Day, D.A., Newburn, M.K., Hu, W., Isaacman-VanWertz, G., Yee, L.D., Thalman, R., Brito, J., Carbone, S., Artaxo, P., Goldstein, A.H., Manzi, A.O., Souza, R.A.F., Mei, F., Shilling, J.E., Springston, S.R., Wang, J., Surratt, J.D., Alexander, M.L., Jimenez, J.L., Martin, S.T., 2017. Influence of urban pollution on the production of organic particulate matter from isoprene epoxydiols in central Amazonia. Atmos. Chem. Phys. 17, 6611–6629. https://doi.org/10.5194/acp-17-6611-2017.

DeCarlo, P.F., Dunlea, E.J., Kimmel, J.R., Aiken, A.C., Sueper, D., Crounse, J., Wennberg, P.O., Emmons, L., Shinozuka, Y., Clarke, A., Zhou, J., Tomlinson, J., Collins, D.R., Knapp, D., Weinheimer, A.J., Montzka, D.D., Campos, T., Jimenez, J.L., 2008. Fast airborne aerosol size and chemistry measurements above Mexico City and Central Mexico during the MILAGRO campaign. Atmos. Chem. Phys. 8, 4027–4048. https://doi.org/10.5194/acp-8-4027-2008.

Decarlo, P.F., Kimmel, J.R., Trimborn, A., Northway, M.J., Jayne, J.T., Aiken, A.C., Gonin, M., Fuhrer, K., Horvath, T., Docherty, K.S., Worsnop, D.R., Jimenez, J.L., 2006. Aerosol mass spectrometer. Anal. Chem. 78, 8281–8289. (Analytical). https://doi.org/8410.1029/2001JD001213.

DeCarlo, P.F., Ulbrich, I.M., Crounse, J., de Foy, B., Dunlea, E.J., Aiken, A.C., Knapp, D., Weinheimer, A.J., Campos, T., Wennberg, P.O., Jimenez, J.L., 2010. Investigation of the sources and processing of organic aerosol over the Central Mexican Plateau from aircraft measurements during MILAGRO. Atmos. Chem. Phys. 10, 5257–5280. https://doi.org/10.5194/acp-10-5257-2010.

Dos Santos, M.J., Silva Dias, M.A.F., Freitas, E.D., 2014. Influence of local circulations on wind, moisture, and precipitation close to Manaus City, Amazon Region, Brazil. J. Geophys. Res. Atmos. 119, 13233–13249. https://doi.org/10.1002/2014JD021969.

Doughty, C.E., Flanner, M.G., Goulden, M.L., 2010. Effect of smoke on subcanopy shaded light, canopy temperature, and carbon dioxide uptake in an Amazon rainforest. Global Biogeochem. Cycles 24, 1–10. https://doi.org/10.1029/2009GB003670.

Draxler, R.R., 2007. Demonstration of a global modeling methodology to determine the relative importance of local and long-distance sources. Atmos. Environ. 41, 776–789. https://doi.org/10.1016/j.atmosenv.2006.08.052.

Dubovik, O., King, M.D., 2000. A flexible inversion algorithm for retrieval of aerosol optical properties from Sun and sky radiance measurements. J. Geophys. Res. 105, 20673. https://doi.org/10.1029/2000JD900282.

Dunlea, E.J., DeCarlo, P.F., Aiken, A.C., Kimmel, J.R., Peltier, R.E., Weber, R.J., Tomlinson, J., Collins, D.R., Shinozuka, Y., McNaughton, C.S., Howell, S.G., Clarke, A.D., Emmons, L.K., Apel, E.C., Pfister, G.G., van Donkelaar, A., Martin, R.V., Millet, D.B., Heald, C.L., Jimenez, J.L., 2009. Evolution of Asian aerosols during transpacific transport in INTEX-B. Atmos. Chem. Phys. 9, 7257–7287. https://doi.org/10.5194/acp-9-7257-2009.

Eidels-Dubovoi, S., 2002. Aerosol impacts on visible light extinction in the atmosphere of Mexico City. In: Science of the Total Environment, pp. 213–220. https://doi.org/10.1016/S0048-9697(01)00983-4.

Farmer, D.K., Matsunaga, A., Docherty, K.S., Surratt, J.D., Seinfeld, J.H., Ziemann, P.J., Jimenez, J.L., 2010. Response of an aerosol mass spectrometer to organonitrates and organosulfates and implications for atmospheric chemistry. Proc. Natl. Acad. Sci. Unit. States Am. 107, 6670–6675. https://doi.org/10.1073/pnas.0912340107.

Fraser, B., 2014. Deforestation: carving up the amazon. Nature 509, 418–419. https://doi.org/10.1038/509418a.

Freney, E.J., Sellegri, K., Canonaco, F., Colomb, A., Borbon, A., Michoud, V., Doussin, J.-F., Crumeyrolle, S., Amarouche, N., Pichon, J.-M., Bourianne, T., Gomes, L., Prevot, A.S.H., Beekmann, M., Schwarzenböeck, A., 2014. Characterizing the impact of urban emissions on regional aerosol particles: airborne measurements during the MEGAPOLI experiment. Atmos. Chem. Phys. 14, 1397–1412. https://doi.org/10.5194/acp-14-1397-2014.

Gabey, A.M., Gallagher, M.W., Whitehead, J., Dorsey, J.R., Kaye, P.H., Stanley, W.R., 2010. Measurements and comparison of primary biological aerosol above and below a tropical forest canopy using a dual channel fluorescence spectrometer. Atmos. Chem. Phys. 10, 4453–4466. https://doi.org/10.5194/acp-10-4453-2010.

Gouw, J.D.E., Jimenez, J.L., 2009. Organic Aerosols in the Earth ' s Atmosphere 43, 7614–7618.

Hallquist, M., Wenger, J.C., Baltensperger, U., Rudich, Y., Simpson, D., Claeys, M., Dommen, J., Donahue, N.M., George, C., Goldstein, A.H., Hamilton, J.F., Herrmann, H., Hoffmann, T., Iinuma, Y., Jang, M., Jenkin, M.E., Jimenez, J.L., Kiendler-Scharr, A., Maenhaut, W., McFiggans, G., Mentel, T.F., Monod, A., Prévôt, a. S.H., Seinfeld, J.H., Surratt, J.D., Szmigielski, R., Wildt, J., 2009. The formation, properties and impact of secondary organic aerosol: current and emerging issues. Atmos. Chem. Phys. 9, 5155–5236. https://doi.org/10.5194/acp-9-5155-2009.

He, X., Li, C.C., Lau, A.K.H., Deng, Z.Z., Mao, J.T., Wang, M.H., Liu, X.Y., 2009. An intensive study of aerosol optical properties in Beijing urban area. Atmos. Chem. Phys. 9, 8903–8915. https://doi.org/10.5194/acp-9-8903-2009.

Heiblum, R.H., Koren, I., Feingold, G., 2014. On the link between Amazonian forest properties and shallow cumulus cloud fields. Atmos. Chem. Phys. 14, 6063–6074. https://doi.org/10.5194/acp-14-6063-2014.

Jolleys, M.D., Coe, H., McFiggans, G., Capes, G., Allan, J.D., Crosier, J., Williams, P.I., Allen, G., Bower, K.N., Jimenez, J.L., Russell, L.M., Grutter, M., Baumgardner, D., 2012. Characterizing the aging of biomass burning organic aerosol by use of mixing ratios: a meta-analysis of four regions. Environ. Sci. Technol. 46, 13093–13102. https://doi.org/10.1021/es302386v.

Joyce, R.J., Janowiak, J.E., Arkin, P.A., Xie, P., Joyce, R.J., Janowiak, J.E., Arkin, P.A., Xie, P., 2004. CMORPH: a method that produces global precipitation estimates from passive microwave and infrared data at high spatial and temporal resolution. J. Hydrometeorol. 5, 487–503. < 0487:CAMTPG > 2.0.CO;2. https://doi.org/10.1175/1525-7541(2004)005.

Kagawa, M., Ishizaka, Y., 2014. Conversion of SO2 to particulate sulfate during transport from China to Japan - assessment by selenium in aerosols -. Aerosol Air Qual. Res. 14, 269–279. https://doi.org/10.4209/aaqr.2012.12.0343.

Kalafut-Pettibone, A.J., Wang, J., Eichinger, W.E., Clarke, A., Vay, S.A., Blake, D.R., Stanier, C.O., 2011. Size-resolved aerosol emission factors and new particle formation/growth activity occurring in Mexico City during the MILAGRO 2006 Campaign. Atmos. Chem. Phys. 11, 8861–8881. https://doi.org/10.5194/acp-11-8861-2011.

Kang, C.-M., Gupta, T., Ruiz, P.A., Wolfson, J.M., Ferguson, S.T., Lawrence, J.E., Rohr, A.C., Godleski, J., Koutrakis, P., 2011. Aged particles derived from emissions of coal-fired power plants: the TERESA field results. Inhal. Toxicol. 23, 11–30. https://doi.org/10.3109/08958371003728040.

Kleinman, L.I., Daum, P.H., Lee, Y.N., Senum, G.I., Springston, S.R., Wang, J., Berkowitz, C., Hubbe, J., Zaveri, R.A., Brechtel, F.J., Jayne, J., Onasch, T.B., Worsnop, D., 2007. Aircraft observations of aerosol composition and ageing in new england and mid-atlantic states during the summer 2002 new england air quality study field campaign. J. Geophys. Res. Atmos. 112, 1–18. https://doi.org/10.1029/2006JD007786.

Kleinman, L.I., Springston, S.R., Daum, P.H., Lee, Y.-N., Nunnermacker, L.J., Senum, G.I., Wang, J., Weinstein-Lloyd, J., Alexander, M.L., Hubbe, J., Ortega, J., Canagaratna, M.R., Jayne, J., 2008. The time evolution of aerosol composition over the Mexico City plateau. Atmos. Chem. Phys. 8, 1559–1575. https://doi.org/10.5194/acp-8-1559-2008.

Kondo, Y., Matsui, H., Moteki, N., Sahu, L., Takegawa, N., Kajino, M., Zhao, Y., Cubison, M.J., Jimenez, J.L., Vay, S., Diskin, G.S., Anderson, B., Wisthaler, A., Mikoviny, T., Fuelberg, H.E., Blake, D.R., Huey, G., Weinheimer, A.J., Knapp, D.J., Brune, W.H., 2011. Emissions of black carbon, organic, and inorganic aerosols from biomass burning in North America and Asia in 2008. J. Geophys. Res. 116, D08204. https://doi.org/10.1029/2010JD015152.

Kuhn, U., Ganzeveld, L., Thielmann, a., Dindorf, T., Schebeske, G., Welling, M., Sciare, J., Roberts, G., Meixner, F.X.X., Kesselmeier, J., Lelieveld, J., Kolle, O., Ciccioli, P., Lloyd, J., Trentmann, J., Artaxo, P., Andreae, M.O.O., 2010. Impact of Manaus city on the amazon Green Ocean atmosphere: ozone production, precursor sensitivity and aerosol load. Atmos. Chem. Phys. 10, 9251–9282. https://doi.org/10.5194/acp-10-9251-2010.

Kulmala, M., Lehtinen, K.E.J., Laaksonen, A., 2006. Cluster activation theory as an explanation of the linear dependence between formation rate of 3nm particles and sulphuric acid concentration. Atmos. Chem. Phys. 6, 787–793. https://doi.org/10.5194/acp-6-787-2006.

Lee, A.K.Y., Willis, M.D., Healy, R.M., Wang, J.M., Jeong, C.H., Wenger, J.C., Evans, G.J., Abbatt, J.P.D., 2016. Single-particle characterization of biomass burning organic aerosol (BBOA): evidence for non-uniform mixing of high molecular weight organics and potassium. Atmos. Chem. Phys. 16, 5561–5572. https://doi.org/10.5194/acp-16-5561-2016.

Lim, S., Lee, M., Kim, S.-W., Yoon, S.-C., Lee, G., Lee, Y.J., 2014. Absorption and scattering properties of organic carbon versus sulfate dominant aerosols at Gosan climate observatory in Northeast Asia. Atmos. Chem. Phys. 14, 7781–7793. https://doi.org/10.5194/acp-14-7781-2014.

Liu, Y., Brito, J., Dorris, M.R., Rivera-Rios, J.C., Seco, R., Bates, K.H., Artaxo, P., Duvoisin, S., Keutsch, F.N., Kim, S., Goldstein, A.H., Guenther, A.B., Manzi, A.O., Souza, R.A.F., Springston, S.R., Watson, T.B., McKinney, K.A., Martin, S.T., 2016. Isoprene photochemistry over the Amazon rainforest. Proc. Natl. Acad. Sci. Unit. States Am. 113, 6125–6130. https://doi.org/10.1073/pnas.1524136113.

Luria, M., Imhoff, R.E., Valente, R.J., Parkhurst, W.J., Tanner, R.L., 2001. Rates of conversion of sulfur dioxide to sulfate in a scrubbed power plant plume. J. Air Waste Manag. Assoc. 51, 1408–1413. https://doi.org/10.1080/10473289.2001.10464368.

Lyamani, H., Olmo, F.J., Alados-Arboledas, L., 2010. Physical and optical properties of aerosols over an urban location in Spain: seasonal and diurnal variability. Atmos. Chem. Phys. 10, 239–254. https://doi.org/10.5194/acp-10-239-2010.

Martin, S.T., Andreae, M.O., Althausen, D., Artaxo, P., Baars, H., Borrmann, S., Chen, Q., Farmer, D.K., Guenther, a., Gunthe, S.S., Jimenez, J.L., Karl, T., Longo, K., Manzi, a., Müller, T., Pauliquevis, T., Petters, M.D., Prenni, a. J., Pöschl, U., Rizzo, L.V., Schneider, J., Smith, J.N., Swietlicki, E., Tota, J., Wang, J., Wiedensohler, a., Zorn, S.R., 2010a. An overview of the amazonian aerosol characterization experiment 2008 (AMAZE-08). Atmos. Chem. Phys. 10, 11415–11438. https://doi.org/10.5194/acp-10-11415-2010.

Martin, S.T., Andreae, M.O., Artaxo, P., Baumgardner, D., Chen, Q., Goldstein, A.H., Guenther, A., Heald, C.L., Mayol-Bracero, O.L., McMurry, P.H., Pauliquevis, T., Pschl, U., Prather, K.A., Roberts, G.C., Saleska, S.R., Silva Dias, M.A., Spracklen, D.V., Swietlicki, E., Trebs, I., 2010b. Sources and properties of Amazonian aerosol particles. Rev. Geophys. 48. https://doi.org/10.1029/2008RG000280.

Martin, S.T., Artaxo, P., Machado, L., Manzi, A.O., Souza, R.A.F., Schumacher, C., Wang, J., Biscaro, T., Brito, J., Calheiros, A., Jardine, K., Medeiros, A., Portela, B., De Sá, S.S., Adachi, K., Aiken, A.C., Alblbrecht, R., Alexander, L., Andreae, M.O., Barbosa, H.M.J., Buseck, P., Chand, D., Comstmstmstock, J.M., Day, D.A., Dubey, M., Fan, J., Faststt, J., Fisch, G., Fortner, E., Giangrande, S., Gilllles, M., Goldststein, A.H., Guenther, A., Hubbbbe, J., Jensen, M., Jimenez, J.L., Keutstsch, F.N., Kim, S., Kuang, C., Laskskin, A., McKinney, K., Mei, F., Millller, M., Nascimento, R., Pauliquevis, T., Pekour, M., Peres, J., Petäjä, T., Pöhlklker, C., Pöschl, U., Rizzo, L., Schmid, B., Shilllling, J.E., Silva Dias, M.A., Smith, J.N., Tomlmlinson, J.M., Tóta, J., Wendisch, M., 2017. The green ocean amazon experiment (GOAMAZON2014/5) observes pollution affecting gases, aerosols, clouds, and rainfall over the rain forest. Bull. Am. Meteorol. Soc. 98, 981–997. https://doi.org/10.1175/BAMS-D-15-00221.1.

Martin, S.T., Artaxo, P., MacHado, L.A.T., Manzi, A.O., Souza, R.A.F., Schumacher, C., Wang, J., Andreae, M.O., Barbosa, H.M.J., Fan, J., Fisch, G., Goldstein, A.H., Guenther, A., Jimenez, J.L., Pöschl, U., Silva Dias, M.A., Smith, J.N., Wendisch, M., 2016. Introduction: observations and modeling of the Green Ocean amazon (GoAmazon2014/5). Atmos. Chem. Phys. 16, 4785–4797. https://doi.org/10.5194/acp-16-4785-2016.

McMeeking, G.R., Bart, M., Chazette, P., Haywood, J.M., Hopkins, J.R., McQuaid, J.B., Morgan, W.T., Raut, J.C., Ryder, C.L., Savage, N., Turnbull, K., Coe, H., 2012. Airborne measurements of trace gases and aerosols over the London metropolitan region. Atmos. Chem. Phys. 12, 5163–5187. https://doi.org/10.5194/acp-12-5163-2012.

Medeiros, A.S.S., Calderaro, G., Guimarães, P.C., Magalhaes, M.R., Morais, M.V.B., Rafee,

S.A.A., Ribeiro, I.O., Andreoli, R.V., Martins, J.A., Martins, L.D., Martin, S.T., Souza, R.A.F., 2017. Power plant fuel switching and air quality in a tropical, forested environment. Atmos. Chem. Phys. 17, 8987–8998. https://doi.org/10.5194/acp-17-8987-2017.

Müller, T., Henzing, J.S., de Leeuw, G., Wiedensohler, A., Alastuey, A., Angelov, H., Bizjak, M., Collaud Coen, M., Engström, J.E., Gruening, C., Hillamo, R., Hoffer, A., Imre, K., Ivanow, P., Jennings, G., Sun, J.Y., Kalivitis, N., Karlsson, H., Komppula, M., Laj, P., Li, S.-M., Lunder, C., Marinoni, A., Martins dos Santos, S., Moerman, M., Nowak, A., Ogren, J.A., Petzold, A., Pichon, J.M., Rodriquez, S., Sharma, S., Sheridan, P.J., Teinilä, K., Tuch, T., Viana, M., Virkkula, A., Weingartner, E., Wilhelm, R., Wang, Y.Q., 2011a. Characterization and intercomparison of aerosol absorption photometers: result of two intercomparison workshops. Atmos. Meas. Tech. 4, 245–268. https://doi.org/10.5194/amt-4-245-2011.

Müller, T., Laborde, M., Kassell, G., Wiedensohler, A., 2011b. Design and performance of a three-wavelength LED-based total scatter and backscatter integrating nephelometer. Atmos. Meas. Tech. 4, 1291–1303. https://doi.org/10.5194/amt-4-1291-2011.

Müller, T., Nowak, A., Wiedensohler, A., Sheridan, P., Laborde, M., Covert, D.S., Marinoni, A., Imre, K., Henzing, B., Roger, J.-C., Martins dos Santos, S., Wilhelm, R., Wang, Y.-Q., de Leeuw, G., 2009. Angular illumination and truncation of three different integrating nephelometers: implications for empirical, size-based corrections. Aerosol Sci. Technol. 43, 581–586. https://doi.org/10.1080/02786820902798484.

Nepstad, D., McGrath, D., Stickler, C., Alencar, A., Azevedo, A., Swette, B., Bezerra, T., DiGiano, M., Shimada, J., Seroa da Motta, R., Armijo, E., Castello, L., Brando, P., Hansen, M.C., McGrath-Horn, M., Carvalho, O., Hess, L., 2014. Slowing Amazon deforestation through public policy and interventions in beef and soy supply chains. Science (80-.) 344, 1118–1123. https://doi.org/10.1126/science.1248525.

Ng, N.L., Herndon, S.C., Trimborn, A., Canagaratna, M.R., Croteau, P.L., Onasch, T.B., Sueper, D., Worsnop, D.R., Zhang, Q., Sun, Y.L., Jayne, J.T., 2011. An aerosol chemical speciation monitor (ACSM) for routine monitoring of the composition and mass concentrations of ambient aerosol. Aerosol Sci. Technol. 45, 780–794. https://doi.org/10.1080/02786826.2011.560211.

Nielsen, I.E., Eriksson, A.C., Lindgren, R., Martinsson, J., Nyström, R., Nordin, E.Z., Sadiktsis, I., Boman, C., Nøjgaard, J.K., Pagels, J., 2017. Time-resolved analysis of particle emissions from residential biomass combustion – emissions of refractory black carbon, PAHs and organic tracers. Atmos. Environ. 165, 179–190. https://doi.org/10.1016/j.atmosenv.2017.06.033.

Oliveira, N. De, Brito, J., Arana, A., Regina, S., Medeiros, B. De, de Oliveira Alves, N., Brito, J., Caumo, S., Arana, A., de Souza Hacon, S., Artaxo, P., Hillamo, R., Teinilä, K., Batistuzzo de Medeiros, S.R., de Castro Vasconcellos, P., 2015. Biomass burning in the Amazon region : aerosol source apportionment and associated health risk assessment. Atmos. Environ. 120, 277–285. https://doi.org/10.1016/j.atmosenv.2015.08.059.

Oliveira, P.H.F., Artaxo, P., Pires, C., De Lucca, S., Procópio, A., Holben, B., Schafer, J., Cardoso, L.F., Wofsy, S.C., Rocha, H.R., 2007. The effects of biomass burning aerosols and clouds on the CO2 flux in Amazonia. Tellus Ser. B Chem. Phys. Meteorol. 59, 338–349. https://doi.org/10.1111/j.1600-0889.2007.00270.x.

Palm, B.B., De Sá, S.S., Day, D.A., Campuzano-Jost, P., Hu, W., Seco, R., Sjostedt, S.J., Park, J.-H., Guenther, A.B., Kim, S., Brito, J., Wurm, F., Artaxo, P., Thalman, R., Wang, J., Yee, L.D., Wernis, R., Isaacman-Vanwertz, G., Goldstein, A.H., Liu, Y., Springston, S.R., Souza, R., Newburn, M.K., Alexander, M.L., Martin, S.T., Jimenez, J.L., 2018. Secondary organic aerosol formation from ambient air in an oxidation flow reactor in central Amazonia. Atmos. Chem. Phys. 467–493. 185194. https://doi.org/10.5194/acp-18-467-2018.

Petzold, A., Schloesser, H., Sheridan, P.J., Arnott, W.P., Ogren, J. a., Virkkula, A., 2005. Evaluation of multiangle absorption photometry for measuring aerosol light absorption. Aerosol Sci. Technol. 39, 40–51. https://doi.org/10.1080/027868290901945.

Petzold, A., Schönlinner, M., 2004. Multi-angle absorption photometry—a new method for the measurement of aerosol light absorption and atmospheric black carbon. J. Aerosol Sci. 35, 421–441. https://doi.org/10.1016/j.jaerosci.2003.09.005.

Pohlker, C., Wiedemann, K.T., Sinha, B., Shiraiwa, M., Gunthe, S.S., Smith, M., Su, H., Artaxo, P., Chen, Q., Cheng, Y., Elbert, W., Gilles, M.K., Kilcoyne, A.L.D., Moffet, R.C., Weigand, M., Martin, S.T., Poschl, U., Andreae, M.O., 2012. Biogenic potassium salt particles as seeds for secondary organic aerosol in the Amazon. Science 337, 1075–1078. https://doi.org/10.1126/science.1223264.

Pöschl, U., Martin, S.T., Sinha, B., Chen, Q., Gunthe, S.S., Huffman, J.A., Borrmann, S., Farmer, D.K., Garland, R.M., Helas, G., Jimenez, J.L., King, S.M., Manzi, A., Mikhailov, E., Pauliquevis, T., Petters, M.D., Prenni, A.J., Roldin, P., Rose, D., Schneider, J., Su, H., Zorn, S.R., Artaxo, P., Andreae, M.O., 2010. Rainforest aerosols as biogenic nuclei of clouds and precipitation in the Amazon. Science 329, 1513–1516. https://doi.org/10.1126/science.1191056.

Ramachandran, S., Rajesh, T.A., 2007. Black carbon aerosol mass concentrations over Ahmedabab, an urban location in western India: comparison with urban sites in Asia, Europe, Canada, and the United States. J. Geophys. Res. Atmos. 112, 1–19. https://doi.org/10.1029/2006JD007488.

Rap, A., Spracklen, D.V., Mercado, L., Reddington, C.L., Haywood, J.M., Ellis, R.J., Phillips, O.L., Artaxo, P., Bonal, D., Restrepo Coupe, N., Butt, N., 2015. Fires increase Amazon forest productivity through increases in diffuse radiation. Geophys. Res. Lett. 42, 4654–4662. https://doi.org/10.1002/2015GL063719.

Reddington, C.L., Butt, E.W., Ridley, D.A., Artaxo, P., Morgan, W.T., Coe, H., Spracklen, D.V., 2015. Air quality and human health improvements from reductions in deforestation-related fire in Brazil. Nat. Geosci. 8, 768–771. https://doi.org/10.1038/ngeo2535.

Rissler, J., Vestin, A., Swietlicki, E., Fisch, G., Zhou, J., Artaxo, P., Andreae, M.O., 2006. Size distribution and hygroscopic properties of aerosol particles from dry-season biomass burning in Amazonia. Atmos. Chem. Phys. 6, 471–491. https://doi.org/10.5194/acp-6-471-2006.

Rizzo, L.V., Artaxo, P., Müller, T., Wiedensohler, A., Paixão, M., Cirino, G.G., Arana, a., Swietlicki, E., Roldin, P., Fors, E.O., Wiedemann, K.T., Leal, L.S.M., Kulmala, M., 2013. Long term measurements of aerosol optical properties at a primary forest site in Amazonia. Atmos. Chem. Phys. 13, 2391–2413. https://doi.org/10.5194/acp-13-2391-2013.

Rizzo, L.V., Correia, A.L., Artaxo, P., Procópio, A.S., Andreae, M.O., 2011. Spectral dependence of aerosol light absorption over \newline the Amazon Basin. Atmos. Chem. Phys. 11, 8899–8912. https://doi.org/10.5194/acp-11-8899-2011.

Russell, P.B., Bergstrom, R.W., Shinozuka, Y., Clarke, A.D., Decarlo, P.F., Jimenez, J.L., Livingston, J.M., Redemann, J., Dubovik, O., Strawa, A., 2010. Absorption Angstrom Exponent in AERONET and related data as an indicator of aerosol composition. Atmos. Chem. Phys. 10, 1155–1169. https://doi.org/10.5194/acp-10-1155-2010.

Sahu, L.K., Kondo, Y., Moteki, N., Takegawa, N., Zhao, Y., Cubison, M.J., Jimenez, J.L., Vay, S., Diskin, G.S., Wisthaler, A., Mikoviny, T., Huey, L.G., Weinheimer, A.J., Knapp, D.J., 2012. Emission characteristics of black carbon in anthropogenic and biomass burning plumes over California during ARCTAS-CARB 2008. J. Geophys. Res. Atmos. 117, D16302. https://doi.org/10.1029/2011JD017401.

Schmid, O., Artaxo, P., Arnott, W.P., Chand, D., Gatti, L.V., Frank, G.P., Hoffer, A., Schnaiter, M., 2006. Physics Spectral Light Absorption by Ambient Aerosols Influenced by Biomass Burning in the Amazon Basin. I : Comparison and Field Calibration of Absorption Measurement Techniques. pp. 3443–3462.

Schuster, G.L., Dubovik, O., Holben, B.N., 2006. Angstrom exponent and bimodal aerosol size distributions. J. Geophys. Res. Atmos. 111, 1–14. https://doi.org/10.1029/2005JD006328.

Sena, E.T., Artaxo, P., Correia, A.L., 2013. Spatial variability of the direct radiative forcing of biomass burning aerosols and the effects of land use change in Amazonia. Atmos. Chem. Phys. 13, 1261–1275. https://doi.org/10.5194/acp-13-1261-2013.

Stein, A.F., Isakov, V., Godowitch, J., Draxler, R.R., 2007. A hybrid modeling approach to resolve pollutant concentrations in an urban area. Atmos. Environ. 41, 9410–9426. https://doi.org/10.1016/j.atmosenv.2007.09.004.

Szmigielski, R., 2013. Chemistry of organic sulfates and nitrates in the urban atmosphere. NATO Sci. Peace Secur. Ser. C Environ. Secur. 120, 211–226. https://doi.org/10.1007/978-94-007-5034-0_17.

Takemura, T., Nakajima, T., Dubovik, O., Holben, B.N., Kinne, S., 2002. Single-scattering albedo and radiative forcing of various aerosol species with a global three-dimensional model. J. Clim. 15, 333–352. < 0333:SSAARF > 2.0.CO;2. https://doi.org/10.1175/1520-0442(2002)015.

Takemura, T., Okamoto, H., Maruyama, Y., Numaguti, A., Higurashi, A., Nakajima, T., 2000. Global three-dimensional simulation of aerosol optical thickness distribution of various origins. J. Geophys. Res. 105, 17853. https://doi.org/10.1029/2000JD900265.

Thalman, R., De Sá, S.S., Palm, B.B., Barbosa, H.M.J., Pöhlker, M.L., Alexander, M.L., Brito, J., Carbone, S., Castillo, P., Day, D.A., Kuang, C., Manzi, A., Ng, N.L., Sedlacek, A.J., Souza, R., Springston, S., Watson, T., Pöhlker, C., Pöschl, U., Andreae, M.O., Artaxo, P., Jimenez, J.L., Martin, S.T., Wang, J., 2017. CCN activity and organic hygroscopicity of aerosols downwind of an urban region in central Amazonia: seasonal and diel variations and impact of anthropogenic emissions. Atmos. Chem. Phys. 17, 11779–11801. https://doi.org/10.5194/acp-17-11779-2017.

Trebs, I., Mayol-Bracero, O.L., Pauliquevis, T., Kuhn, U., Sander, R., Ganzeveld, L., Meixner, F.X., Kesselmeier, J., Artaxo, P., Andreae, M.O., 2012. Impact of the Manaus urban plume on trace gas mixing ratios near the surface in the Amazon Basin: implications for the NO-NO_2-O $_3$ photostationary state and peroxy radical levels. J. Geophys. Res. Atmos. 117, 1–16. https://doi.org/10.1029/2011JD016386.

Tunved, P., Partridge, D.G., Korhonen, H., 2010. New trajectory-driven aerosol and chemical process model Chemical and Aerosol Lagrangian Model (CALM). Atmos. Chem. Phys. 10, 10161–10185. https://doi.org/10.5194/acp-10-10161-2010.

Wang, J., Krejci, R., Giangrande, S., Kuang, C., Barbosa, H.M.J., Brito, J., Carbone, S., Chi, X., Comstock, J., Ditas, F., Lavric, J., Manninen, H.E., Mei, F., Moran-Zuloaga, D., Pöhlker, C., Pöhlker, M.L., Saturno, J., Schmid, B., Souza, R.A.F., Springston, S.R., Tomlinson, J.M., Toto, T., Walter, D., Wimmer, D., Smith, J.N., Kulmala, M., Machado, L.A.T., Artaxo, P., Andreae, M.O., Petäjä, T., Martin, S.T., 2016. Amazon boundary layer aerosol concentration sustained by vertical transport during rainfall. Nature 539, 416–419. https://doi.org/10.1038/nature19819.

Weber, R.J., Sullivan, A.P., Peltier, R.E., Russell, A., Yan, B., Zheng, M., de Grouw, J., Warneke, C., Brock, C., Holloway, J.S., Atlas, E.L., Edgerton, E., 2007. A study of secondary organic aerosol formation in the anthropogenic-influenced southeastern United States. J. Geophys. Res. Atmos. 112, 1–13. https://doi.org/10.1029/2007JD008408.

Whitehead, J.D., Darbyshire, E., Brito, J., Barbosa, H.M.J., Crawford, I., Stern, R., Gallagher, M.W., Kaye, P.H., Allan, J.D., Coe, H., Artaxo, P., McFiggans, G., 2016a. Biogenic cloud nuclei in the central Amazon during the transition from wet to dry season. Atmos. Chem. Phys. 16, 9727–9743. https://doi.org/10.5194/acp-16-9727-2016.

Whitehead, J.D., Darbyshire, E., Brito, J., Barbosa, H.M.J., Crawford, I., Stern, R., Gallagher, M.W., Kaye, P.H., Allan, J.D., Coe, H., Artaxo, P., McFiggans, G., 2016b. Biogenic cloud nuclei in the central Amazon during the transition from wet to dry season. Atmos. Chem. Phys. 16, 9727–9743. https://doi.org/10.5194/acp-16-9727-2016.

Zhou, J., Swietlicki, E., Hansson, H.C., Artaxo, P., 2002. Submicrometer aerosol particle size distribution and hygroscopic growth measured in the Amazon rain forest during the wet season. J. Geophys. Res. Atmos. 107. https://doi.org/10.1029/2000JD000203.